SPECTRAL EFFICIENCY IMPROVEMENT OF LOW PEAK-TO-AVERAGE POWER RATIO COMPLETE COMPLEMENTARY CODE DIVISION MULTIPLE ACCESS SYSTEM

by

Frederick Hendrik de Lange

Submitted in partial fulfilment of the requirements for the degree
Master of Engineering (Electronic Engineering)

in the

Department of Electrical, Electronic and Computer Engineering
Faculty of Engineering, Built Environment and Information Technology

UNIVERSITY OF PRETORIA

July 2018

SUMMARY

SPECTRAL EFFICIENCY IMPROVEMENT OF LOW PEAK-TO-AVERAGE POWER RATIO COMPLETE COMPLEMENTARY CODE DIVISION MULTIPLE ACCESS SYSTEM

by

Frederick Hendrik de Lange

Supervisor: Prof. L.P. Linde

Co-supervisor: Dr. J.H. van Wyk

Department: Electrical, Electronic and Computer Engineering

University: University of Pretoria

Degree: Master of Engineering (Electronic Engineering)

Keywords: Code division multiple access, Complete complementary codes, Multicarrier, Peak-to-average power ratio, spectral efficiency.

An investigation into the peak-to-average power ratio (PAPR) performance of cyclic rotation complete complementary code division multiple access (CR-CC-CDMA) has been conducted. Additionally, a novel orthogonal signalling technique, referred to as complementary rotation keying (CRK), has been developed for improving the spectral efficiency (SE) of CC-CDMA whilst maintaining a low PAPR. The CRK system is based on the concept of CR of CC codes in order to allow interoperability with CR-CC-CDMA systems. To this end, both systems employ a similar transmitter and receiver structure.

The CR-CC-CDMA technique suffers from increased PAPR as SE per user is increased. The CRK system offers an improvement in SE, while maintaining the PAPR of a CC-CDMA system. The bit error rates of both systems were unaffected in a joint system, indicating complete interoperability. This allows dynamic adjustment of the PAPR and SE of any user in the system, with users being able to switch between both systems without causing multi user interference.

OPSOMMING

SPEKTRALE EFFEKTIWITEITS-VERBETERING VAN LAE PIEK-TOT-GEMIDDELDE DRYWINGSVERHOUDING VOLLEDIG KOMPLEMENTÊRE KODE VERDELING VEELVULDIGE TOEGANG STELSEL

deur

Frederick Hendrik de Lange

Studieleier: Prof. L.P. Linde

Mede-studieleier: Dr. J.H. van Wyk

Departement: Elektriese, Elektroniese en Rekenaar-ingenieurswese

Universiteit: Universiteit van Pretoria

Graad: Magister in Ingenieurswese (Elektroniese Ingenieurswese)

Sleutelwoorde: Kode-verdeling-veelvuldige-toegang, Multidraer, Piek-tot-gemiddelde drywingsverhouding, spektrale effekiwiteit, Volledig komplementêre kodes.

‘n Ondersoek na die piek-tot-gemiddelde drywingsverhouding (PAPR) van sikliese rotasie volledig komplementêre kodeverdeling-veelvuldige-toegang (CR-CC-CDMA) is onderneem. Verder is ‘n nuwe ortogonale sleuteling tegniek, naamlik komplementêre rotasie sleuteling (CRK), ontwikkel om die spektrale effektiwiteit (SE) van ‘n CC-CDMA stelsel te verbeter sonder om die PAPR te affekteer. Die CRK stelsel is ontwikkel gebaseer op die CR van CC kodes om samewerking met CR-CC-CDMA stelsels te verseker. Vir hierdie rede gebruik beide stelsels ’n soortgelyke sender - en ontvangerstruktuur.

Die CR-CC-CDMA tegniek lei aan verhoogde PAPR met verhoogings in SE per gebruiker. Die CRK bied ’n verbetering in die SE en behou die PAPR van die CC-CDMA stelsel. Die bis foutwaarskynlikheid van beide stelsels was onveranderd in ’n geïntegreerde stelsel, wat daarop dui dat voledige samewerking tussen die stelsels bereik is. Dit laat dinamiese verstelling van die PAPR en SE per gebruiker toe wat daartoe lei dat gebruikers tussen beide stelsels kan skakel sonder om multi-gebruiker steuring te veroorsaak.

ACKNOWLEDGEMENTS

The author would like to thank his study leaders, Prof. L.P. Linde and Dr. J.H. van Wyk, as well as Dr. K. Dhuness, for their guidance and support.

Thanks to CeTEIS, our industry partners (Telkom SA and Bytes Universal Systems (previously UNISYS South Africa)) and the National Research Foundation for their financial support towards CeTEIS, for granting the opportunity to conduct this research.

To my fellow student, P. Jansen van Vuuren, A. Jansen van Vuuren, N. de Figueiredo, N. van der Neut, and all others, who shared ideas, laughs and cries.

I would also like to thank my friends and family for their continued support.

LIST OF ABBREVIATIONS

3GPP	3rd Generation Partnership Project
ACE	Active constellation extension
AWGN	Additive white Gaussian noise
BER	Bit error rate
BPSK	Binary phase shift keying
BW	Bandwidth
CC	Complete complementary
CCC	Complete complementary code
CCDF	Complementary cumulative distribution function
CDMA	Code division multiple access
CE	Constant envelope
CP	Cyclic prefix
CR	Cyclic rotation
CRK	Complementary rotation keying
CCSK	Cyclic code shift keying
DFT	Discrete Fourier transform
DS	Direct sequence
FDMA	Frequency division multiple access
FFT	Fast Fourier transform
FT	Fourier transform
GBF	Generalized Boolean function
GDJ	Golay Davis Jedwab
GSM	Global system for mobile communications
IFFT	Inverse fast Fourier transform
ISI	Inter-symbol interference
LTE	Long term evolution
MC	Multicarrier
MOCS	Mutually orthogonal complementary set
MUI	Multi-user interference
OFDM	Orthogonal frequency division multiplexing
OFDMA	Orthogonal frequency division multiple access
PA	Power Amplifier
PAPR	Peak-to-average power ratio

PG	Processing gain
POCS	Projection onto convex sets
PPC	Pulse position code
P/S	Parallel to serial
QAM	Quadrature amplitude modulation
QPSK	Quadrature phase shift keying
RM	Reed Muller
SC	Single carrier
SE	Spectral efficiency
SF	Spreading factor
SGP	Smart gradient projection
SLM	Selected mapping
SNR	Signal-to-noise ratio
S/P	Serial to parallel
TDMA	Time division multiple access
TETRA	Terrestrial trunked radio
TI	Tone insertion
TR	Tone reservation
UMTS	Universal mobile telecommunication system

LIST OF SYMBOLS

b_v	Modulation symbol per sequence for DS-CDMA and MC-CDMA
b_v^{QPSK}	QPSK modulated symbol per flock for CRK
$\hat{b}_v^{QPSK}$	Recovered QPSK modulated symbol per flock for CRK
b_v^r	Modulation symbol per data sub-stream for CR-CC-CDMA
$\hat{b}_v^r$	Recovered modulation symbol per data sub-stream for CR-CC-CDMA
$\hat{b}_v^r$	Decision device inputs for CRK
$\boldsymbol{C}_v$	Spreading matrix for CC-CDMA
$\boldsymbol{C}_v^r$	Cyclic rotated spreading matrix for CR-CC-CDMA and CRK
$\boldsymbol{c}_v$	Spreading sequence for CDMA
D	Real number used for TI
$\boldsymbol{d}_v[k]$	Data stream per flock for CC-CDMA
$\widehat{\boldsymbol{d}}_v[k]$	Recovered data stream per flock for CC-CDMA
$\boldsymbol{d}_v^{CRK}[k]$	Position data sub-stream per flock for CRK
$\widehat{\boldsymbol{d}}_v^{CRK}[k]$	Recovered position data sub-stream per flock for CRK
$\boldsymbol{d}_v^{QPSK}[k]$	Data symbol data sub-stream per flock for CRK
$\widehat{\boldsymbol{d}}_v^{QPSK}[k]$	Recovered data symbol data sub-stream per flock for CRK
$\boldsymbol{d}_v^r[k]$	Data sub-stream per rotation for CR-CC-CDMA
$\widehat{\boldsymbol{d}}_v^r[k]$	Recovered data sub-stream per rotation for CR-CC-CDMA
$\delta[\tau]$	Kronecker delta function
ε	Roots of unity
${\varepsilon_n}^v$	SNR scaling factor
k	Bit index in data stream
k_{CK}	Number of bits modulated onto correlation position for CK or CCSK
k_{CRK}	Number of bits modulated onto correlation position for CRK
k_v^r	Number of bits per data sub-stream for CR-CC-CDMA
L	Length of spreading sequence used for DS-CDMA and MC-CDMA
L_{CP}	Length of cyclic prefix in OFDM and similar multicarrier modulation techniques
L_E	Length of element sequence used in CC-CDMA
L_F	Length of frequency domain spreading factor for MC-DS-CDMA
L_{SF}	Total spreading factor for MC-DS-CDMA and CC-CDMA
L_T	Length of time domain spreading factor for MC-DS-CDMA

l	Column index of element of spreading sequence for CC-CDMA
M	Number of element sequences in a flock
m	Row index of element sequence in a flock
N	Number of elements in a discrete signal
N_{ACT}	Number of active subcarriers in OFDM of similar multicarrier modulation techniques
N_{FFT}	Length of FFT and IFFT used for OFDM or similar multicarrier modulation techniques
n_f	Element index in discrete frequency signal
n_t	Element index in discrete time signal
$\boldsymbol{n}_{PAPR}$	Subset of subcarriers used for PAPR reduction in tone insertion or tone reservation
$P[n_t]$	Instantaneous signal power
P_{AVE}	Average Signal Power
P_{CLP}	PAPR reduction power clipping level
$PAPR_{CLP}$	PAPR reduction clipping level
$PAPR_{THR}$	PAPR reduction threshold
p	Integer value used for TI
q	Integer value used for TI
R	Number of rotations used in CR-CC-CDMA
r	Rotation index for CR-CC-CDMA and CRK
$\hat{r}$	Recovered rotation index for CRK
$\boldsymbol{s}_v^l[n]$	Time domain signal block per time slot for CC-CDMA
$\hat{\boldsymbol{s}}_v^l[n]$	Received time domain signal block per time slot for CC-CDMA
$\theta(\boldsymbol{c}_a, \boldsymbol{c}_b)(\tau)$	Correlation between $\boldsymbol{c}_a$ and $\boldsymbol{c}_b$
τ	Time shift between signals
μ	SGP scaling factor of ACE
V	Number of flocks of sequences in an MOCS
v	Flock index for CC-CDMA
v	Code index for DS-CDMA and MC-CDMA
$X[n_f]$	Discrete frequency domain symbol
$X_{diff}[n_f]$	Difference frequency domain symbol for PAPR reduction
$\boldsymbol{X}_v$	Frequency domain symbol per flock for CC-CDMA
$\widehat{\boldsymbol{X}}_v$	Recovered frequency domain symbol per flock for CC-CDMA

$\boldsymbol{X}_v^r$	Frequency domain spread matrix per rotation for CR-CC-CDMA
$X_v^{SLM}[n_t]$	Phase vectors for SLM
$x(t)$	Continues time signal
$x[n_t]$	Discrete time signal
$x_{diff}[n_t]$	Difference signal for PAPR reduction
$\widehat{\boldsymbol{x}}_v^m[r]$	Correlator outputs for CC-CDMA
$Y[n_f]$	Modified OFDM symbol for PAPR reduction
$y[n_t]$	Modified OFDM time signal for PAPR reduction
$\boldsymbol{y}_v^l[n]$	Transmission time domain signal block per column for CC-CDMA
$\widehat{\boldsymbol{y}}_v^l[n]$	Received transmission time domain signal block per column for CC-CDMA

TABLE OF CONTENTS

LIST OF FIGURES

CHAPTER 1 INTRODUCTION

1.1 CHAPTER OVERVIEW

The problem addressed in this research is described in Section 1.2. The research objectives and questions are stated in Section 1.3. The approach followed in this research is described in Section 1.4. The research goals are listed in Section 1.5. The research contributions are covered in Section 1.6. The research outputs are listed in Section 1.7.

1.2 PROBLEM STATEMENT

1.2.1 Context of the problem

Access to information is considered a human right [1, 2]. Mobile data networks are a major enabler of such access. However, for many people living in rural areas of developing countries, such as South Africa, access to mobile data networks is not readily available [3, 4].

As mobile data networks are operated for profit, such networks can only be deployed where economically viable. This requires a minimum number of users to be supported per cost incurred for such a network. Thus, in order to improve the economic viability of an area either the number of users available must be increased, or the equipment cost must be decreased. Given that rural areas have very low, non-varying population densities, the number of users can only be increased by increasing the area covered by the same equipment. By increasing the area covered by a network, or reducing the costs of the network, it is possible that an area can become economically viable enough for a network operator to provide services to that area.

Low peak-to-average power ratio (PAPR) systems can be implemented to achieve the increase in viability by either increasing the area covered, or by decreasing the cost of the equipment used. Many low PAPR systems have several drawbacks. It is thus necessary to use a low-PAPR system with additional properties best suited to the required application.

Code division multiple access (CDMA) is the foundation of the universal mobile telecommunication system (UMTS) [5]. As a multiple access scheme, it allows support of multiple users. CDMA is a spread spectrum technology, which mitigates channel effects such as narrow band jamming and fast fading. The CDMA technology implemented in the UMTS resulted in multi-user interference (MUI), resulting in severe performance degradation when supporting multiple users.

Multi-carrier (MC) communication techniques have been adopted in most state of the art communication systems, such as IEEE 802.11 [6] and the long term evolution (LTE) of the Universal Mobile Telecommunication System (UMTS) [7]. MC communication provides robust protection against many channel effects common in mobile communication. MC communication systems are often based on orthogonal frequency division multiplexing (OFDM). MC communication and CDMA can also be combined into different configurations, allowing for greater flexibility in optimising a system for a particular application.

Complete complementary codes (CCCs) are a type of sequence that can be used for CDMA, without resulting in MUI [8]. CCCs are derived from Golay complementary pairs of sequences, originally developed for spectrometry [9]. CCCs supports fewer users than CDMA or other conventional transmission systems. Conventional complete complementary (CC)-CDMA systems also only support a limited spectral efficiency (SE) per user, although techniques have been developed to increase the SE to be comparable to conventional transmission systems [8, 10]. CCCs thus provide the advantages of CDMA, while mitigating some of the disadvantages. CC-CDMA systems can also be configured to have properties of a MC communication system.

CCCs have been shown to have the property of very low PAPR when the element sequences are used as codewords for OFDM. The complementary properties of the sequences are lost when used in this way.

1.2.2 Research gap

Although some research has been performed with regards to the improvement of SE of CC-CDMA systems, none of this research has investigated the PAPR implications of using techniques for improving the SE of the CC-CDMA systems, or the development of a low PAPR CC-CDMA system with increased SE.

1.3 RESEARCH OBJECTIVE AND QUESTIONS

The purpose of this research is to determine if it is possible to design a CC-CDMA system with an improved SE while maintaining a lower PAPR than current state-of-the-art MC communication systems. The research questions are listed below:

- What is the PAPR performance of existing techniques for improving SE in CC-CDMA systems?
- Can a CC-CDMA system be designed with an improved SE?
- Can a CC-CDMA system with improved SE maintain a lower PAPR than current state-of-the-art MC communication systems?
- What is the bit error rate (BER) performance of a CC-CDMA system using a low PAPR CCC?

1.4 APPROACH

A CC-CDMA system model was developed and simulated using low PAPR CCCs. The communication system features an existing, as well as, a novel technique in order to increase the SE of the system. The PAPR and BER performance of the system was simulated with different design parameters and compared to baseline systems representative of state-of-the-art MC communication systems.

1.5 RESEARCH GOALS

The goal of this research is to design a low PAPR CC-CDMA system with improved SE, which is also configurable to different user requirements, without degradation of BER

performance. Additionally, this research will investigate the PAPR performance of existing techniques used to increase the SE of CC-CDMA systems.

1.6 RESEARCH CONTRIBUTION

Contributions of this research are:

1. Investigation into the PAPR performance of existing techniques used for increasing the SE of a CC-CDMA system.
2. Development of a technique to improve the SE of a CC-CDMA system while maintaining a low PAPR.
3. Simulation of the PAPR performance of the CC-CDMA system utilising technique in (2).
4. Simulation of the BER performance of the CC-CDMA system utilising technique in (2).

1.7 RESEARCH OUTPUTS

The following research output was submitted for publication:

1. F.H. de Lange, J.H. van Wyk, L.P. Linde, "Spectral Efficiency Improvement of Low Peak-to-Average Power Ratio Complete Complementary CDMA Systems", *Telecommunication Systems*, submitted Feb 2018.

1.8 OVERVIEW OF STUDY

In Chapter 2 an overview of the relevant literature is given. In Chapter 3 the mathematical foundation related to the work conducted in this research is presented. In Chapter 4 the system models used for this research are presented. In Chapter 5 the experimental method used for generating the results in this research is presented. In Chapter 6 the PAPR and BER results of both configurations are presented. In Chapter 7 the results are discussed and interpreted in greater detail. In Chapter 8 conclusions are drawn from the results and future work proposed.

CHAPTER 2 LITERATURE STUDY

2.1 CHAPTER OVERVIEW

An overview of the most relevant literature related to the work performed in the research is presented in this chapter. As this research combines the topics of PAPR and CDMA, each is presented in a separate section. Multiple access is introduced in Section 2.2. MC communication systems are covered in Section 2.3. PAPR is addressed in Section 2.4. Orthogonal keying is described in Section 2.5. CDMA is covered in Section 2.6.

2.2 MULTIPLE ACCESS

Multiple access is used to share transmission resources between several users. In time division multiple access (TDMA), different timeslots are allocated to different users. This is the simplest form of multiple access. TDMA is used in systems such as GSM and TETRA. TDMA requires guard intervals between timeslots to protect against MUI caused by time dispersion.

In frequency division multiple access (FDMA), users are allocated different carrier frequencies. This is the equivalent of having multiple systems in parallel, each on a separate sub-carrier frequency. However, in FDMA, all users are demodulated using the same carrier frequency, and de-multiplexed in the baseband.

2.3 MULTICARRIER COMMUNICATION

2.3.1 Multicarrier communication

MC communication has become popular in wireless communication applications [6, 7]. MC communication offers improved spectral efficiency and improved robustness to harsh transmission channels with minimal increase in complexity. The greatest disadvantage of using MC communication is an inherently high PAPR. The high PAPR is a result of the multiple independent signals that are summed together to generate the MC signal. The variance of the signal increases with the number of subcarriers used, as described by the central limit theorem [11].

2.3.2 Orthogonal frequency division multiplexing

OFDM is a special case of FDMA, where the different carriers have minimum separation while remaining orthogonal. This allows for maximum SE. The OFDM signal is modulated using the inverse fast Fourier transform (IFFT), with the sampling frequency chosen to adhere to the required bandwidth (BW). OFDM, as with other MC techniques, suffers from a very high PAPR. For practical implementations, a cyclic prefix (CP) is added, which is a certain number of the time domain samples at the end of an OFDM signal that are duplicated and appended to the front of the signal. The CP is added in order to mitigate multipath channel effects. The number of samples in the CP is chosen to be one fewer than the number of paths in the impulse response of the channel. When a CP is used, the received signal, given by the convolution of the channel impulse response with the OFDM time signal, prefixed by the CP, yields the circular convolution of the channel impulse response with the original OFDM time signal. The circular convolution may be transformed using the Fourier Transform (FT) in order to allow less complex signal processing to be used to recover the transmitted signal. The significant parameters in OFDM are the Fast Fourier Transform (FFT) size N_{FFT}, the number of active subcarriers, N_{ACT}, where $N_{ACT} \leq N_{FFT}$, the cyclic prefix length L_{CP} and the sampling frequency. Multiple users are accommodated in OFDM using timeslots as in TDMA. For more flexible distribution of resources between users, more complex multiple access configurations can be employed, using time slots per subcarrier. This is known as orthogonal FDMA (OFDMA).

2.3.2.1 Orthogonal frequency division multiple access

In OFDMA, the signal is modulated using the IFFT, similar to OFDM. However, users can be allocated different subsets of subcarriers, using different subsets of timeslots within each allocated subcarrier, allowing OFDMA to support many users with different throughput requirements. This does however require a continuous feedback control channel to allocate these resources per user. OFDMA is used in the LTE of the UMTS, standardized within the 3rd Generation Partnership Project (3GPP) [7].

2.3.2.2 Discrete Fourier transform spread orthogonal frequency division multiplexing

In order to address the high PAPR of OFDM systems, discrete Fourier transform (DFT) precoding has been employed in some OFDM systems. The DFT precoding is done by multiplying each data symbol by a different row of the DFT matrix. This creates a spread spectrum system. The main advantage of DFT spread (DFT-s) OFDM systems is that conventional OFDMA systems can be easily converted as the DFT-s OFDM system only required a DFT/inverse DFT (IDFT) pair in addition to the OFDMA system. For this reason, DFT-s OFDM is implemented in the uplink of LTE, as OFDMA is implemented in the downlink. This allows both the uplink and downlink to share a similar architecture. DFT-s OFDM systems can be configured in two different ways, depending on how the frequency domain symbols are mapped to the OFDMA system's subcarriers. In localized DFT-s OFDM, symbols are mapped to adjacent subcarriers. Localized DFT-s OFDM has the potential for higher SE, as each user can be assigned a block of subcarriers, where that user's channel has optimal channel gain. In distributed DFT-s OFDM, symbols are assigned to subcarriers throughout the entire BW of the system. In particular, when subcarriers are evenly spaced, the system is referred to as interleaved DFT-s OFDM. Distributed DFT-s OFDM systems offer the potential for frequency diversity, as the system provides some protection against frequency selective fading. Distributed DFT-s OFDM offers lower PAPR than the localized configuration, however only localised DFT-s OFDM is used in LTE, as distributed DFT-s OFDM cannot easily configure for users with different data rate requirements [12]. DFT-s OFDM can be considered as a MC-CDMA system per user, where the data for all subcarriers per user is spread over the entire BW for that user, with multiple access between the users still implemented through OFDMA.

2.4 PEAK-TO-AVERAGE POWER RATIO

The PAPR of a signal $x(t)$ is defined as the ratio between the peak instantaneous power over an interval of time, *t*, where $t_0 \leq t \leq t_1$ and the average power of the signal over the same time frame,

$$PAPR(x(t)) = \frac{\max_{t_0}^{t_1}(|x^2(t)|)}{\int_{t_0}^{t_1}|x^2(t)|dt\,/(t_1 - t_0)} \tag{2.1}$$

[13]. The PAPR is an indication of the variance in the power of the signal. A signal with unitary PAPR is referred to as a constant envelope (CE) signal, as this is only possible if the signal has a constant power envelope. CE signals have the best PAPR characteristics. Many single carrier (SC) systems have CE signals. MC type systems often have much higher PAPR values. PAPR values are often expressed in decibels (dB). Therefore, a CE signal would have a PAPR of 0 dB. An example of the PAPR of a sinusoid and a normally distributed random signal are shown in Fig. 2.1 and Fig. 2.2.

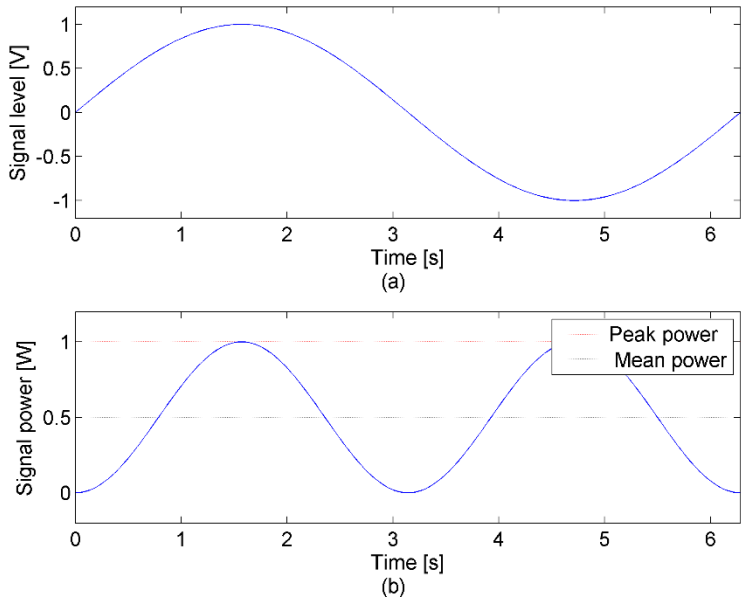

Figure 2.1. PAPR of sinusoid.

(a) Voltage signal. (b) Power signal.

It should be observed from Fig. 2.2 that the normally distributed signal has significant variations in power levels, far greater than the sinusoid shown in Fig. 2.1. The sinusoid therefore has a significantly lower PAPR value than the normally distributed signal. Signals with large PAPR values can cause power amplifiers (PAs) to be driven into saturation, leading to in-band and out-of-band distortion. If an amplified signal would

become distorted, the power of the input signal can be attenuated in order to reduce the peak power sufficiently to avoid distortion. This process is referred to as PA back-off. PA-back-off reduces the peak power of the signal, but also reduces the mean power of the signal, thereby reducing the BER performance of the system. Low PAPR signals can be operated closer to the PA saturation point without risk of saturation.

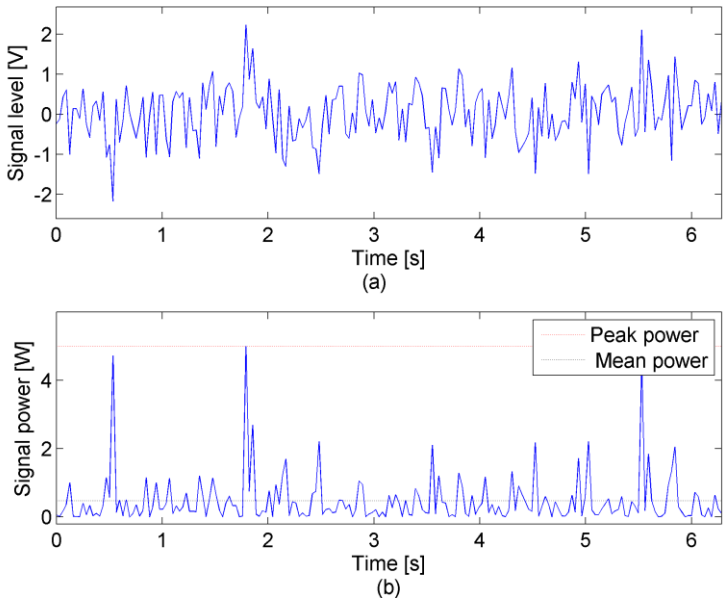

Figure 2.2. PAPR of random signal.

(a) Voltage signal. (b) Power signal.

Examples of PA back-off for low and high PAPR signals are shown below in Fig. 2.3 to Fig. 2.4. In Fig. 2.3 PA back-off is applied to the high PAPR signal, thereby reducing its peak power to the same level as the low PAPR signal. It can be seen that the high PAPR signal has a significantly lower mean power than the low PAPR signal. This will cause severe loss in the system performance. In Fig. 2.4 no PA back-off is applied to the high PAPR signal. It can be seen that while both the signals have the same mean power level, the high PAPR signal has a peak power level significantly higher than the 1 dB saturation point of the amplifier. This will result in significant distortion of the output signal that will cause severe degradation of the spectral characteristics of the transmitter signal.

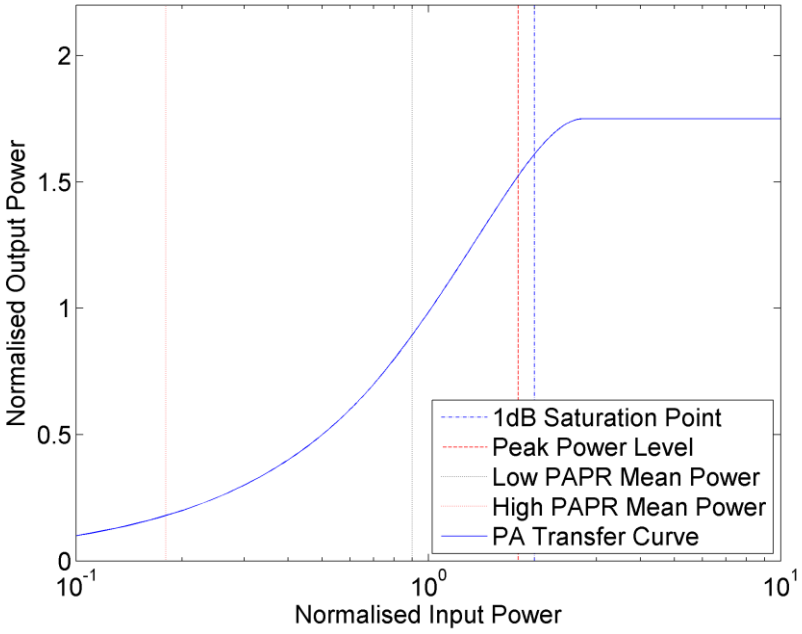

Figure 2.3. Amplification of signals with the same peak power. Mean power levels of low and high PAPR signals with the same peak power shown on amplifier transfer curve.

Multiple access can increase the PAPR of a system, as multiple independent signals are added together before transmission. This phenomenon is more prevalent in the downlink. However, in the downlink, the increased PAPR can be mitigated by the use of expensive transmission equipment with higher power ratings. An example of this is seen in LTE, where DFT-s OFDM is only used in the uplink to address PAPR, but not in the downlink [7].

For telecommunication systems in rural areas, reduction of the PAPR results in multiple ways in which the cost effectiveness of a specific area can be improved. As a reduced PAPR allows a system to operate at a higher average power, the transmission range can be increased. This allows an operator to provide service to more customers using the same equipment. Alternatively, in areas where the range cannot be increased, or where regulatory requirements do not allow for an increase in transmitted power, a reduced PAPR allows the same average power to be achieved with a reduced peak power. The reduced peak power allows the system to be operated with an amplifier with reduced power rating.

This decreases the cost of the equipment required to provide service to a specific area. This can be beneficial in both rural, as well as urban areas.

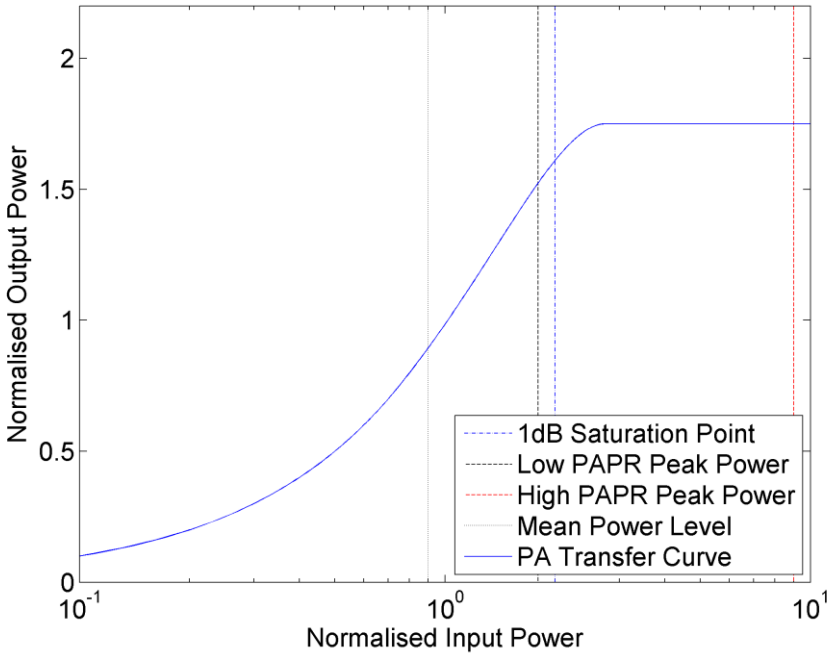

Figure 2.4. Amplification of signals with the same mean power. Peak power levels of low and high PAPR signals with the same mean power shown on amplifier transfer curve. Note peak power level of high PAPR signal in saturation region of amplifier.

2.4.1 Peak-to-average power ratio reduction techniques

As PAPR is the most significant disadvantage to using MC communication techniques, multiple techniques have been developed to improve the PAPR of a MC communication system [14]. These techniques all offer different trade-offs in terms of complexity, PAPR reduction performance, transmission overhead and BER performance degradation. The most widely used techniques are described in the following subsections.

2.4.1.1 Clipping and Filtering

In clipping and filtering, an amplitude clipping function is applied to the OFDM time signal $x[n_t] = IFFT(X[n_f])$ [15]. The clipped signal samples (elements), $x'[n_t]$, are given by

$$x'[n_t] = \begin{cases} x[n_t] & , \quad if\ P[n_t] \leq P_{CLP} \\ x[n_t] \times \frac{\sqrt{P_{CLP}}}{|x[n_t]|}, & if\ P[n_t] > P_{CLP} \end{cases} \quad \forall n, \tag{2.2}$$

where $P[n_t]$ is the instantaneous signal power,

$$P[n_t] = x[n_t] \times x^*[n_t], \tag{2.3}$$

P_{CLP} is the clipping power level,

$$P_{CLP} = PAPR_{CLP} \times P_{AVE}, \tag{2.4}$$

and P_{AVE} is the average signal power,

$$P_{AVE} = \frac{1}{N}\sum_{n=1}^{N} P[n_t]. \tag{2.5}$$

Clipping ensures that the maximum PAPR does not exceed P_{CLP}. Clipping does however result in severe in-band and out-of-band components.

Filtering can be applied after clipping. Filtering does reduce the out-of-band distortion, but results in peak regrowth, therefore no longer ensuring the maximum PAPR. Clipping and filtering have minimal complexity, but multiple iterations are required to achieve good PAPR reduction performance. In-band distortion can lead to severe BER degradation. Clipping and filtering does not decrease the data transmission rate.

2.4.1.2 Active Constellation Extension

In active constellation extension (ACE), an OFDM time signal $x[n_t]$ is evaluated in terms of its PAPR [16]. If the PAPR is higher than the PAPR threshold $PAPR_{THR}$, a temporary time signal is generated. There are two techniques for generating the temporary signal. In repeated clipping all elements with power above the clipping power level are reduced to the clipping level, using (2.2).

Alternatively, in repeated enlipping (enhancement and clipping) all non-zero elements' magnitudes are scaled to the clipping level using a scaling function,

$$x'[n_t] = \begin{cases} 0, & if\ x[n_t] = 0 \\ x[n_t] \times \frac{\sqrt{P_{CLP}}}{|x[n_t]|}, & otherwise \end{cases} \forall n. \tag{2.6}$$

A difference signal $x_{diff}[n_t]$ is generated between the temporary and original signal. This difference signal shows where the original signal should be altered in order to reduce the PAPR. The difference signal is projected back into the frequency domain by means of a FFT. This generates a difference OFDM symbol, $X_{diff}[n_t]$. The difference OFDM symbol is compared to the original OFDM symbol. If an element in the difference OFDM symbol is in the same quadrant as the corresponding element in the original OFDM symbol $X[n_f]$, the element is kept. All other elements in the difference OFDM symbol are made zero. In projection onto convex sets (POCS) ACE, the difference OFDM symbol is added to the original OFDM symbol to create a modified OFDM symbol $Y[n_f]$ [17]. In smart gradient projection (SGP) ACE, the difference symbol is first scaled by a factor μ that improves PAPR reduction without resulting in peak regrowth, before being added to the original OFDM symbol. The result is that the modified symbol will have some modified constellation points with a greater magnitude than the original OFDM symbol. The modified constellation points will thus fall in the decision region of the original constellation points without reducing the minimum distance between the constellation points, as is seen in Fig. 2.5.

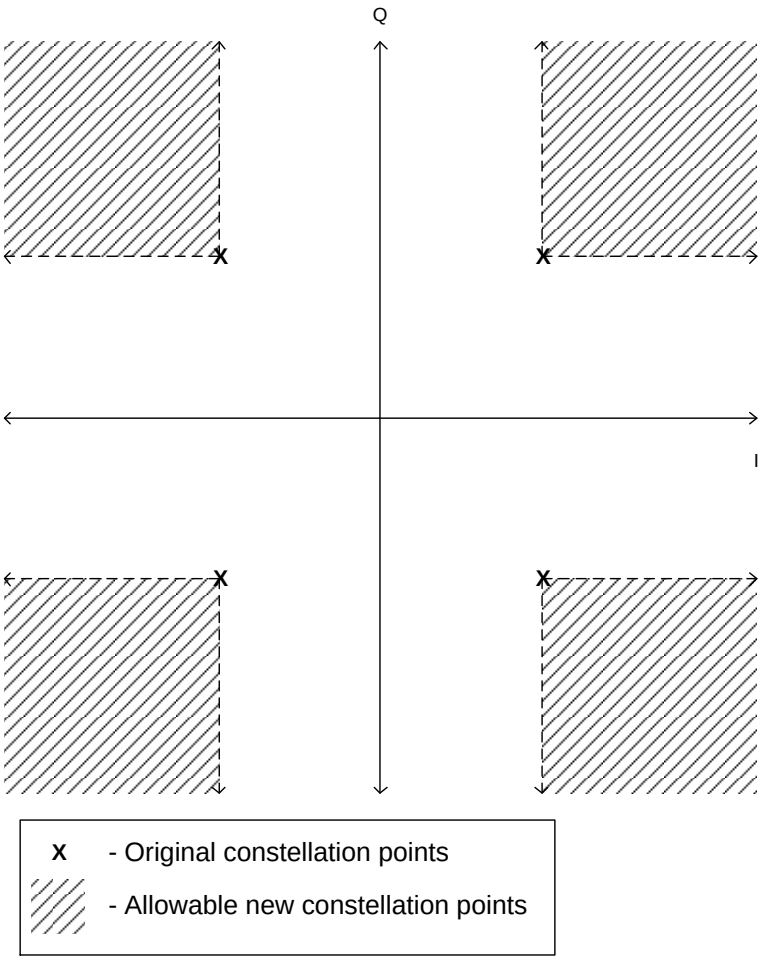

Figure 2.5. Allowable constellation points for ACE (adapted from, [14] © IEEE 2005).

For larger constellation sizes, only the outer-most constellation points can be adjusted to improve the PAPR. This leads to reductions in the improvement in the PAPR. The modified symbol is transformed into the time domain by an IFFT. If the modified OFDM time signal $y[n_t]$ has a lower PAPR than the original signal, it is kept. If not, it is discarded. This process can be repeated recursively for greater PAPR reduction performance, at the cost of computational complexity. ACE yields the greatest PAPR reduction with no requirement for transmission overhead. ACE does result in greatly increased complexity for multiple iterations and does result in minimal increase in BER.

2.4.1.3 Tone Reservation and Tone Insertion

In tone reservation (TR) several of the subcarriers in an OFDM symbol $X[n_f]$ are kept zero [18]. These subcarriers are known as the set of peak reduction subcarriers $\boldsymbol{n}_{PAPR}$, with

$$X[n_f] = 0, n \in \boldsymbol{n}_{PAPR}. \tag{2.7}$$

If the PAPR of the time signal $x[n_t]$ exceeds the PAPR threshold $PAPR_{THR}$, a temporary time signal is generated, with all power peaks reduced to the clipping power level using (2.2). A difference OFDM signal is generated between the temporary and original signal. The difference signal is projected back into the frequency domain by means of an FFT. This generates a difference OFDM symbol $X_{diff}[n_f]$. Elements in the difference OFDM symbol corresponding to the reserved elements are then added to the original OFDM symbol to create a modified OFDM symbol,

$$Y[n_f] = \begin{cases} X[n_f], & n_f \notin \boldsymbol{n}_{PAPR} \\ X_{diff}[n_f], & n_f \in \boldsymbol{n}_{\boldsymbol{P}APR}. \end{cases} \tag{2.8}$$

The new symbol is transformed into the time domain by an IFFT. If the modified OFDM time signal has a lower PAPR than the original signal, it is kept. If not, it is discarded.

In tone insertion (TI), if the PAPR of the time signal $x[n_t]$ exceeds $PAPR_{THR}$, the original constellation points on one or more subcarriers are mapped to several different constellation points in a new, expanded constellation [18]. This mapping function is given by:

$$Y[n_f] = X[n_f] + p \times D + j \times q \times D, n_f \in \boldsymbol{n}_{PAPR}, \tag{2.9}$$

where p,$q \in \mathbb{Z}$, $D \in \mathbb{R}^+$ and $\boldsymbol{n}_{PAPR}$ is the subset of subcarriers used for PAPR reduction. The values of p and q are modified in order to find the greatest PAPR reduction. The receiver requires a modulo-D operator after symbol detection in order to de-map the expanded constellation back to the original constellation points. The expanded constellation also results in an increase in transmitter power.

2.4.1.4 Selected Mapping

In selected mapping (SLM), if the PAPR of the time signal $x[n_t]$ exceeds the PAPR threshold $PAPR_{THR}$, the original OFDM symbol $X[n]$ is multiplied by several predefined phase vectors $X_v^{SLM}[n_f]$ [19]. Modified OFDM symbols are all transformed to the time domain through the IFFT. The resulting time signals are compared, and the signal with the best PAPR is selected. SLM required the transmission of side information to indicate which phase vector was selected, which results in a reduction in SE. SLM requires significant signal processing resources, as multiple IFFTs are required. The PAPR reduction performance and PAPR reduction complexity increase with the number of phase vectors available.

2.4.2 Comparison of PAPR reduction techniques

A comparison of the PAPR reduction techniques for OFDM, as described in Section 2.3.1, as well as other low PAPR systems, is provided in Table 2.1.

Table 2.1. Comparison of PAPR reduction techniques. ACE and distributed DFT-s OFDM can be considered for use in communication systems in rural areas.

Technique	PAPR decrease	SE decrease	Complexity	BER degradation
Clipping and filtering	Minimal	None	Minimal	Substantial
ACE	Substantial	None	Substantial	Minimal
Tone reservation	Average	Minimal	Minimal	None
Tone insertion	Average	None	Average	Minimal
SLM	Average	Average	Substantial	None
Localized DFT-s OFDM	Average	None	Minimal	None
Distributed DFT-s OFDM	Substantial	Minimal	Average	None

From Table 2.1 it should be observed that the most popular PAPR reduction techniques provide PAPR reduction at some cost. This is an inherent trade-off in attempting to modify the characteristics of an existing system. It is thus desirable to have a system with an inherent low PAPR, so as to not require additional operations in order to lower the PAPR of the system. As ACE and distributed DFT-s OFDM provide the greatest PAPR reduction, these techniques would be competing techniques for providing data services in rural areas, although both have significant drawbacks making them less than ideal.

2.5 ORTHOGONAL KEYING

In orthogonal keying systems, all possible transmission signals are chosen from a set of orthogonal symbols. The transmission data are then mapped to each of the possible symbols. This results in only a single symbol being transmitted at a time. This is in contrast to systems such as OFDM, where independent data are modulated on each of the orthogonal subcarriers. Orthogonal keying systems offer an improvement in BER over conventional systems such as BPSK but typically suffer from low SE. In some orthogonal keying systems, an additional modulation symbol can be modulated onto the transmission signal. This results in a slight recovery of SE, although generally not enough to compensate for the lost SE from using orthogonal keying [11].

2.5.1 Frequency shift keying

Frequency shift keying (FSK) is an orthogonal keying system, where the orthogonal symbols used for transmission are orthogonal subcarriers. FSK can be directly compared to OFDM, with FSK mapping data to an individual subcarrier rather than to all subcarriers. As FSK only transmits a single subcarrier at a time, it has many of the properties of a SC system.

2.5.2 Code keying

In code keying (CK), orthogonal sequences are used as the symbols for transmission. These sequences can be implemented in the time domain or the frequency domain, leading to increased flexibility in implementation. As the sequences are used as codewords without

additional modulation, the sequences can be chosen to have desirable properties, such as low PAPR or error correcting capabilities [20, 21].

2.6 CODE DIVISION MULTIPLE ACCESS

CDMA is a multiple access technology that is used to either allow simultaneous transmission by several users on the same frequency spectrum at the same time or to allow enhanced detection in harsh channel conditions. The latter is possible due to the processing gain (PG) of the sequences used. The PG results from the fact that a correlator is used at the receiver. By integrating the elements of the spread signal over the symbol period, the signal level at the detection device is larger than for a conventional signal. The elements in a spreading sequence, as well as in a spread signal, are referred to as chips. When using real sequences, the PG is equal to L (the length of the sequences used, i.e. the number of chips in the spreading sequence). For complex sequences, the PG is twice the length of the sequence. There are several different implementations used for CDMA. CDMA systems require greater bandwidth than conventional communication systems per user, however, the system bandwidth can be same as other communication systems. This is because the users share the same frequency spectrum.

2.6.1 Direct sequence code division multiple access

In direct sequence CDMA (DS-CDMA), users are allocated different orthogonal spreading sequences. The users' data are then spread using their respective sequences, by multiplying their data symbols with each chip in the spreading sequence, and occupy a bandwidth significantly larger than the original data (approximately equal to the sum of the bandwidths required for all users). The ratio of the spread bandwidth to original bandwidth is referred to as the spreading factor (SF) of the system. The users transmit their data using the same frequency band, at the same time. Signal detection at the receiver is performed through correlation. The BER performance of a DS-CDMA system is limited by MUI in time dispersive channels. DS-CDMA is used in the wideband-CDMA (WCDMA) air interface of the 3GPP UMTS. In WCDMA, Walsh-Hadamard sequences (often referred to only as Walsh sequences) are used for multiple access, as Walsh sequences offer variable

SFs within a signal set of sequences, allowing them to be used to spread users with different data rate requirements to the same overall bandwidth. The autocorrelation of a length 8 Walsh sequence is shown in Fig. 2.6.

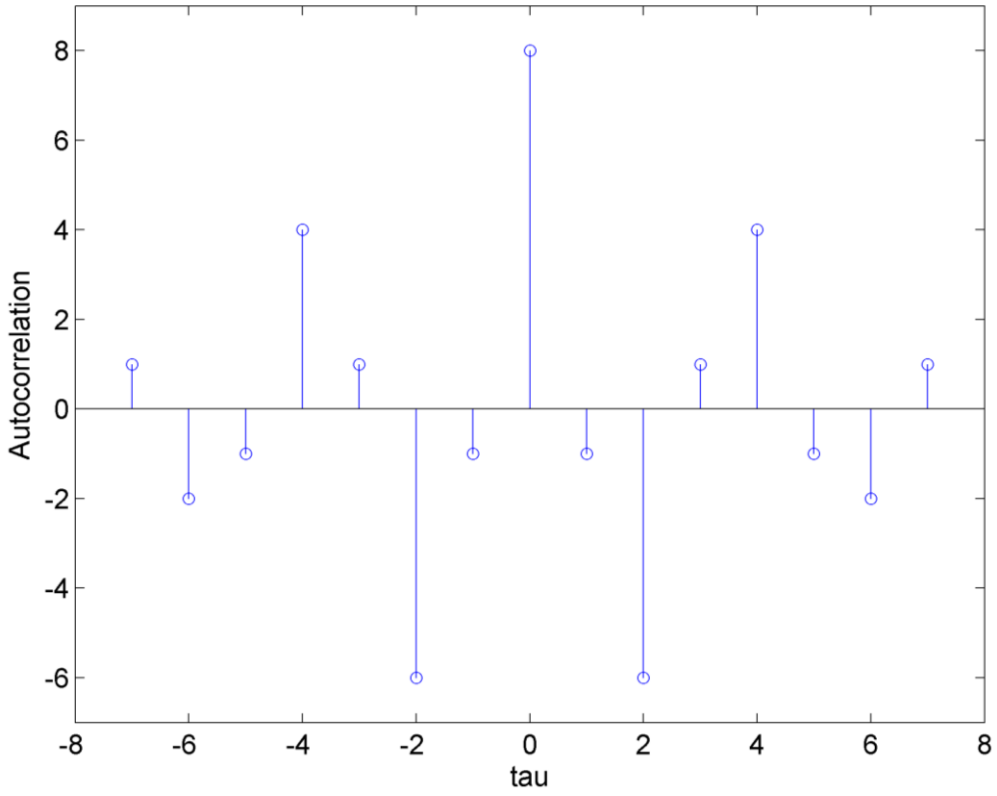

Figure 2.6. Walsh sequence autocorrelation.

In Fig. 2.6 it should be observed that the autocorrelation of Walsh sequences have several non-zero elements at non-zero time shifts, referred to as a side lobes. This will result in BER degradation if the received signal contains any time shifted versions of the transmitted signal, such as echoes in a multipath channel. The cross-correlation between two different Walsh sequences is shown in Fig. 2.7. It should be observed that the cross-correlation between the Walsh sequences has several side lobes. These non-zero elements will result in BER degradation of users which are not synchronised, or if a user's received signal contains any time shifted versions of another user's transmitted signal.

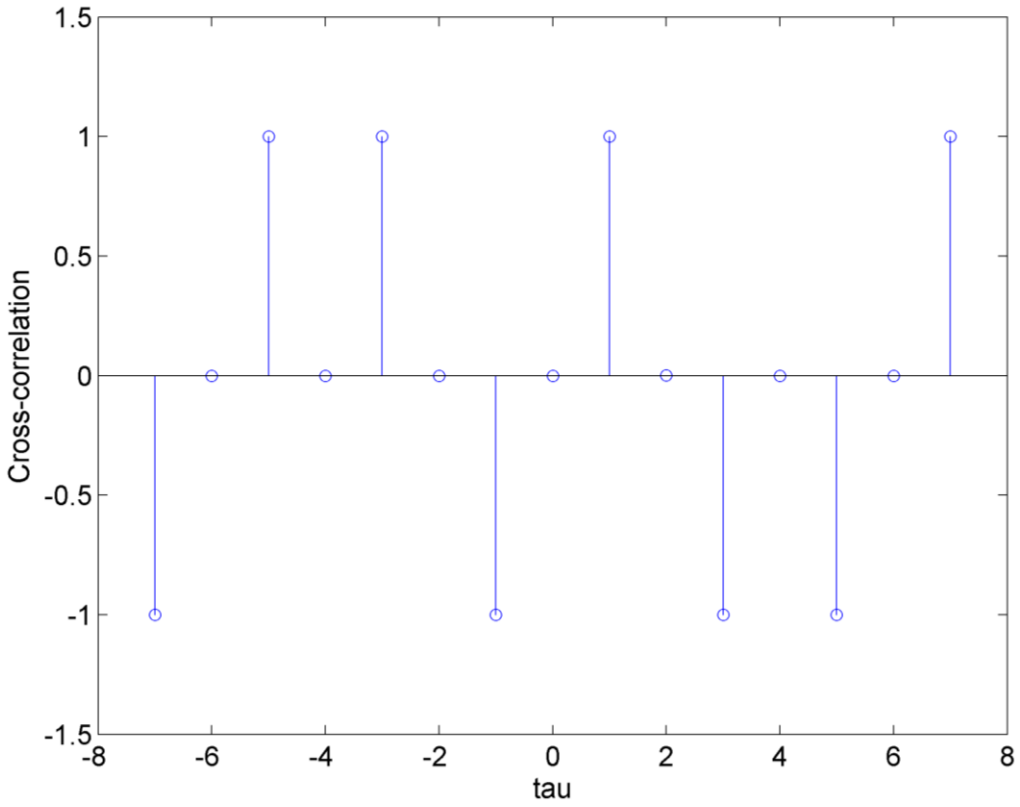

Figure 2.7. Cross-correlation between Walsh sequences.

2.6.2 Multicarrier and direct-sequence multicarrier code division multiple access

In MC-CDMA, user data are spread as in DS-CDMA. However, the spread signal is mapped to different subcarriers. The mapped signal is used as the input of an OFDM system. This results in the spreading taking place in the frequency domain. Multiple data symbols can each be spread in parallel, and combined before OFDM modulation, as they are orthogonal due to the spreading. As MC-CDMA is a MC technology, it also suffers from a high PAPR in the uplink. In the downlink, the PAPR is higher still, as the different users' signals are superimposed before transmission.

In MC-DS-CDMA, each subcarrier in an MC-CDMA system is spread using a time domain spreading sequence. MC-DS-CDMA has more design parameters, allowing more flexibility when designing for different transmission environments. MC-DS-CDMA can be seen as a generalization of DS-CDMA and MC-CDMA, as both systems can be

described using MC-DS-CDMA, with either the time domain SF L_T (for MC-CDMA) or frequency domain SF L_F (for DS-CDMA) set to 1. MC-DS-CDMA can also be used to describe TDMA and FDMA when the orthogonal sequences used are pulse position codes (PPCs, described in Section 3.2), and L_F or L_T are set to 1 respectively. MC-DS-CDMA also has a high PAPR as it is a MC technology. MC-DS-CDMA does however have a lower PAPR than MC-CDMA with the same total SF

$$L_{SF} = L_F \times L_T, \tag{2.10}$$

as MC-DS-CDMA has fewer subcarriers, with some of the spreading performed in the time domain [22]. When comparing MC-DS-CDMA to other CDMA techniques, it is important that the total SF L_{SF} is the same for both systems.

2.6.3 Cyclic code shift keying

Cyclic code shift keying (CCSK) is a special case of CK. Cyclic code shift keying is a technique for improving the SE of systems when low PAPR is a high priority. CCSK is used in MC systems using polyphase sequences. Polyphase sequences have inherently low PAPR when used in MC systems [21, 23, 24]. Additionally, polyphase sequences are known to be orthogonal with all cyclic shifts of the base sequence. Thus all the orthogonal symbols can be generated from one polyphase sequence.

In CCSK, data are modulated on the choice of sequence used, rather than being spread by the sequences as in conventional CDMA. The number of bits that can be transmitted per symbol, k_{CR}, is dependent on the length of the sequences used, defined as:

$$k_{CK} = log_2(L). \tag{2.11}$$

Additionally, a conventional modulation symbol such as binary phase shift keying (BPSK), quadrature phase shift keying (QPSK) or M-ary quadrature amplitude modulation (M-QAM) can be modulated onto the transmitted sequence, allowing for a slight increase in transmission rate. For BPSK, the system is then known as cyclic shift bi-orthogonal keying. For QPSK, the system is known as QPSK-CCSK. In a polyphase based system, the

entire set of sequences have to be used for a single user, reducing the number of users that can be supported to one. [21]

2.6.4 Complete complementary code division multiple access

Complete complementary CDMA (CC-CDMA) differs from conventional CDMA as the spreading is performed with a matrix rather than a vector, as in the case of an individual (unitary) sequence [8, 25]. The matrix is known as a flock of sequences, with each row or column representing an element sequence. It is also possible for an element sequence to consist of a two-dimensional matrix [26]. Users' data are spread using all element sequences from the same flock of sequences. It is necessary for all element sequences to be transmitted independently. At the receiver, the element sequences are correlated individually. The outputs of the receiver correlators for each element sequence in a flock are added together, as can be seen in Fig. 2.8.

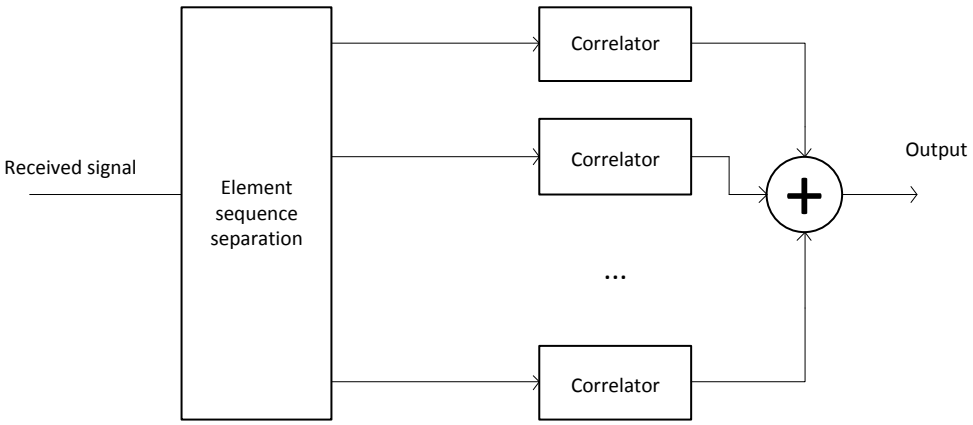

Figure 2.8. Complete complementary code correlation.

The sum produces a correlator output with a single peak at zero shift, and no side lobes. This is known as the Kronecker delta function $\delta[t]$, and is considered a perfect autocorrelation, as time-shifted versions of the signal will not produce inter-symbol interference (ISI). The element sequences have to be transmitted independently in order to avoid creating cross correlation between the element sequences. There are multiple ways in which the element sequences of a flock can be separated. The methods conventionally used are based on TDMA or FDMA, with the element sequences separated in the time domain or frequency domain. In these cases, each element sequence is spread over the frequency

domain or time domain respectively. As flocks of element sequences cannot be described by unitary sequences, CC-CDMA cannot be described in terms of MC-DS-CDMA, although it has been mistakenly referred to as such in literature [13, 27]. CC-CDMA systems suffers from a greatly reduced SE, as each user is spread by M sequences, but only a small number of users (V) can be supported ($V \leq M$). The overall maximum SE of an CC-CDMA system is $1/L_E$, with L_E the length of the element sequences used. To mitigate this significant reduction in SE, offset stacking or cyclic rotation CC-CDMA (CR-CC-CDMA) have been employed to improve the SE of an CC-CDMA system. When comparing CC-CDMA to other CDMA techniques, it is important that the total SF, L_{SF} ,

$$L_{SF} = L_E \times M, \tag{2.12}$$

is the same for both systems. As CC-CDMA differs significantly from conventional CDMA systems based on unitary sequences, there are several definitions that are important when working with CC-CDMA sequences [8, 13]:

i) Auto-complementary set: a set (flock) of sequences that result in a perfect autocorrelation when the autocorrelation function of the element sequences in the set are summed together;

ii) Cross-complementary sets: two sets (flocks) of sequences that result in perfect cross-correlation when the cross-correlation between the corresponding element sequences are summed together;

iii) Mutually orthogonal complementary sets (MOCSs): two or more auto-complementary sets (flocks) that are all cross-complementary among each other;

iv) CC set: a set of MOCSs (flocks) where the number of sets (flocks) is equal to the maximum number of possible sets (flocks), ($V = M$).

Golay sequences have been shown to have a PAPR of 2 (3 dB) when used in code-keying (CK) OFDM [28]. In this application, individual sequences are used as codewords and are not used in pairs or sets for their complementary properties. By using the sequences as codewords, the PAPR of 3 dB can be maintained, which is not possible when the sequences are used in a flock. A method for generating Golay sequences from cosets of the

first order Reed Muller (RM) code within the second order RM code has been developed in [20]. The sequences generated by this method are referred to as Golay Davis Jedwab (GDJ) sequences. The use of Reed-Muller codes for the generation allows the use of GDJ sequences as codewords to be efficiently generated and decoded for use in CK OFDM. Additionally, this allows the codewords to have intrinsic error correction capabilities. The PAPR of a CK OFDM system utilizing GDJ sequences will be at most 2 (3dB) [28]. Additional cosets of the second order RM code can be included, or a single coset can be used for generation of the utilized sequences, resulting in a trade-off between PAPR, code-rate and the minimum distance of the codewords. An analytical proof that GDJ sequences will have a PAPR of 2 (3dB) when used as codewords in CK OFDM has been presented in [20]. Additionally, a graph based method has been developed for generation of CCs [29]. A method for generation of a set of CCCs using RM codes has been developed in [30], which allows efficient generation of CCCs for use in CC-CDMA systems.

2.6.4.1 Offset stacking and cyclic rotation complete complementary code division multiple access

Offset stacking is a technique used to improve the SE of CC-CDMA systems [8]. Offset stacking takes advantage of the perfect correlator output, by transmitting new data every chip, rather than every symbol. As the correlator only has an output at zero-shift, the additional transmitted data do not cause ISI in additive white Gaussian noise (AWGN). ISI will however occur in a time dispersive channel, as echoes of a sequence will interfere with a delayed version of itself. Offset stacking can achieve a maximum system SE of 1 symbol/s/Hz (sym/s/Hz), the same as OFDM and conventional CDMA. Users with different SE requirements can also be supported. Offset stacking can however only be used when the element sequences are spread in the time domain. Offset stacking also requires signal processing to be performed at the chip rate, which can be very high in broadband applications, leading to increased power consumption. An example of an offset stacking system is shown in Fig. 2.9 over two symbol periods. Only one element sequence from a

flock is shown, although the process will be repeated for all element sequences. As is required for offset stacking, the element sequences are spread in the time domain.

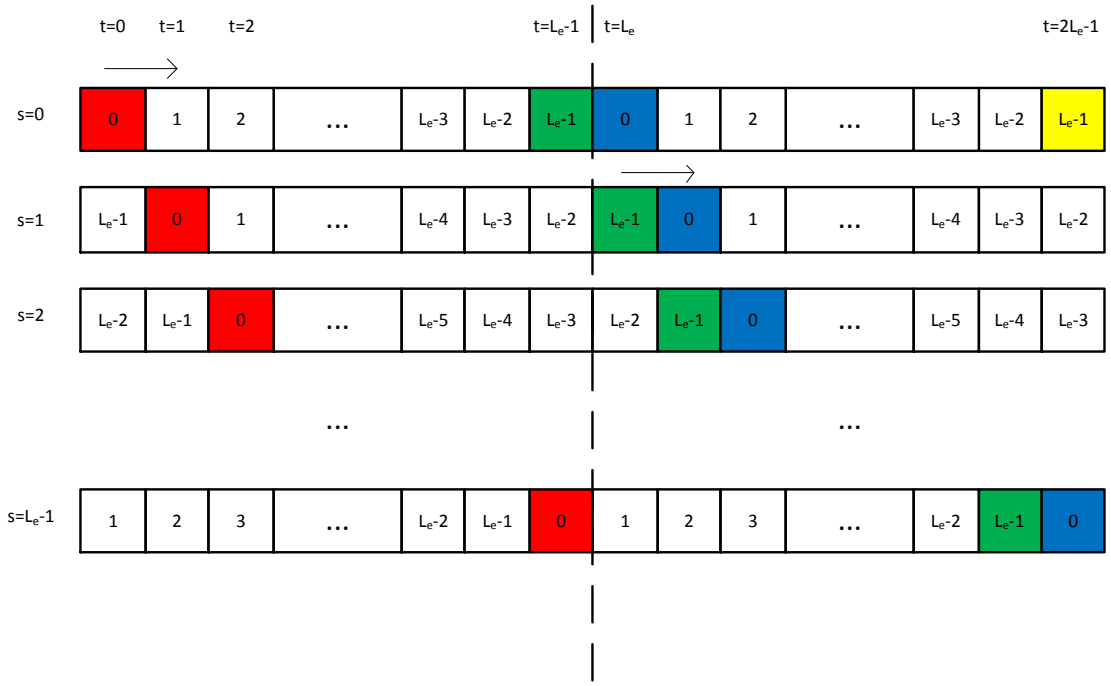

Figure 2.9. Offset staking system operation depicting two spread symbols of length $\boldsymbol{L_E}$ at different time offsets. Red and green rectangles represent the first and last chip of the first symbol. Blue and yellow rectangle represent the first and last chip of the second symbol. The overlap between the two symbols should be noted.

At $s = 0$, the first symbol is represented by the chips red to green. The second symbol is represented by the chips blue to yellow. At $s = 1$, the first symbol is offset by one chip duration. This results in overlap between the second symbol (t=0) and the shifted first symbol ($s = 1$). At $s = 2$, the first symbol is offset by an additional chip duration. This results in further overlap. This procedure is continued until $s = L_e - 1$, at which point the next symbol is placed at $s = 0$ again. Correlation is performed on the signal every chip duration. Thus, frame synchronization is not required.

CR-CC-CDMA is an alternative technique for increasing the SE of CC-CDMA systems [10]. As with offset stacking, CR-CC-CDMA takes advantage of the perfect correlator output of CC-CDMA. In CR-CC-CDMA, element sequences are each cyclically shifted, in

order to produce a larger set of sequences. Each rotated version of a flock of element sequences is then used as a new flock of sequences, through which new data can be spread. An example of a CR-CC-CDMA system is shown in Fig. 2.10 over two symbol periods. Only one element sequence from a flock is shown, although the process will be repeated for all element sequences. In this example, the element sequences are spread in the time domain in order to be comparable to offset stacking.

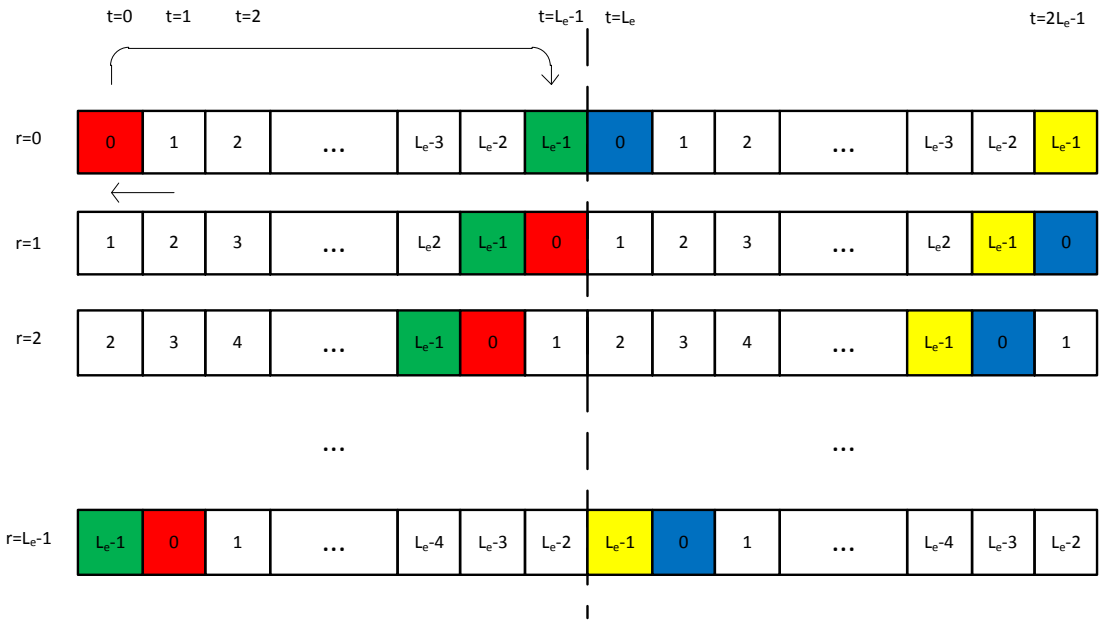

Figure 2.10. CR-CC-CDMA system operation depicting two spread symbols of length $\boldsymbol{L_E}$ for different rotation indexes. Red and green rectangles represent the first and last chip of the first symbol. Blue and yellow rectangle represent the first and last chip of the second symbol. The lack of overlap between the two symbols should be noted.

At $r = 0$, the first symbol is represented by the chips red to green and the second symbol is represented by the chips blue to yellow (as in Fig. 2.9). This is the unrotated version of the element sequences, denoted as rotation 0. At $r = 1$, the first symbols start with the second chip of the first symbol of $r = 0$. This is denoted as rotation 1. The procedure is repeated for the second symbol. Owing to the block-wise nature of this technique, there is no overlap between the first and second symbols. At $r = 2$, both symbols start with the third

chip of the symbols of $r = 0$. This is denoted as rotation 2. This process is repeated until $r = L_e - 1$ where both symbols start with the last chip of the symbols of $r = 0$.

CR-CC-CDMA can be used with element sequences that are spread in either the time domain or the frequency domain. In CR-CC-CDMA, correlation is performed using periodic correlation, allowing all rotations of an element sequence to be detected with a single operation. This resulted in signal processing taking place at the symbol rate, reducing power consumption. CR-CC-CDMA does however require frame synchronization, in order to ensure that the first chip in a symbol is in the correct position. The PAPR performance of offset stacking and CR-CC-CDMA has not yet been investigated. This is significant as both systems are both multicarrier and multiple access schemes, and as such, could have a significantly high PAPR.

2.6.4.2 Low peak-to-average power ratio complete complementary codes

A family of CCCs with low PAPR properties has been developed based on the generation of sequences using RM codes [13]. When the low PAPR CCCs' element sequences are each spread over time, with each element sequence on a different OFDM subcarrier, the PAPR of each column sequence will be at most 2 (3dB) after the IFFT. The low PAPR property is achieved by introduction of quadratic terms of the row index into the generation function. This results in each column sequence being a GJD sequence. The elements of the sequences are roots of unity, i.e.

$$\varepsilon = e^{j2\pi/q}, \tag{2.13}$$

with $q \geq 2$ the alphabet size. As the chips of the element sequences in this set of CCCs have to be separated in the time domain in order to achieve the low PAPR property, both offset stacking and CR-CC-CDMA can be used to significantly improve the SE of the system, although both would result in an increase in PAPR. As the sequences have an inherently low PAPR, CRK can also be used to maintaining the low PAPR property, whilst improve the system SE, although less than for offset stacking or CR-CC-CDMA.

2.7 CHAPTER OVERVIEW

The most relevant literature has been presented in order to provide a sufficient frame of reference for analysis of this research. The significance of the PAPR problem has been explained as motivation for this research. Also, of significance importance are the techniques of orthogonal keying and CR-CC-CDMA, as these techniques are investigated in following chapters.

CHAPTER 3 FUNDAMENTAL CONCEPTS

3.1 CHAPTER OVERVIEW

The fundamental concepts related to this research are presented in this chapter. This includes the mathematical foundation for the presented techniques as well as important concepts pertaining to practical systems, as they relate to this research. This is particularly important as PAPR is fundamentally a practical problem. Correlation is analysed in Section 3.2. Power amplifiers are covered in Section 3.3. Complementary rotation keying is described in Section 3.4.

3.2 CORRELATION

An important function in signal processing is correlation. Discrete signals can be represented as vectors, with each sample representing an element in the vector. This allows signals to be processed through vector algebra. Correlation is performed by determining the inner product between two vectors representing two signals. Correlation determines if two signals can be represented using a mutual base signal [11]. Base signals are often simple signals used to represent several signals, in order to compare properties of the original signals. The set of orthogonal sinusoids represented in the DFT are an example of base signals used for correlation. The aperiodic correlation between two complex-valued sequences $\boldsymbol{c}_a$ and $\boldsymbol{c}_b$ of length N is given by:

$$\theta(\boldsymbol{c}_a, \boldsymbol{c}_b)(\tau) = \begin{cases} \sum_{t=0}^{N-1-\tau} c_a[n_t] \times (c_b[n_t + \tau])^*, & 0 \leq \tau \leq (N-1); \\ \sum_{t=0}^{N-1+\tau} c_a[n_t - \tau] \times (c_b[n_t])^*, & -(N-1) \leq \tau \leq -1; \\ 0, & |\tau| \geq N \end{cases} \tag{3.1}$$

The correlation between two signals is referred to as the cross-correlation between those signals. The projection of a signal onto other signal in signal space is determined through their cross-correlation. The correlation of a signal with itself, $\theta(\boldsymbol{c}_a, \boldsymbol{c}_a)$, is referred to as the autocorrelation of the signal. The autocorrelation of a signal shows how a signal projects onto time-shifted versions of itself.

An important subset of signals are those for which $\theta(\boldsymbol{c}_a, \boldsymbol{c}_b)(0) = 0$. These signals are orthogonal to each other, and in terms of telecommunication systems, cannot cause interference with each other. An example of an orthogonal sequence set is PPCs. PPCs are defined as the rows of an identity matrix. A set of length 4 PPCs are:

$$\boldsymbol{c}_0 = [1, 0, 0, 0]$$
$$\boldsymbol{c}_1 = [0, 1, 0, 0]$$
$$\boldsymbol{c}_2 = [0, 0, 1, 0]$$
$$\boldsymbol{c}_3 = [0, 0, 0, 1].$$

The set of length 4 PPCs, along with their sum, is shown in Fig. 3.1. It should be observed that transmission of multiple codes at the same time will not cause interference among each other. The vectors representing the signals exist in a multidimensional signal space, where each signal is orthogonal to the other signals. In a communication system using these PPCs, each sequence $\boldsymbol{c}_r$ could be multiplied by some complex modulation symbol b_v, in this example $b_v = 1$, for all v. Two bits of binary data could also be used to select a single sequence as codeword to be transmitted. This would be an example of orthogonal keying.

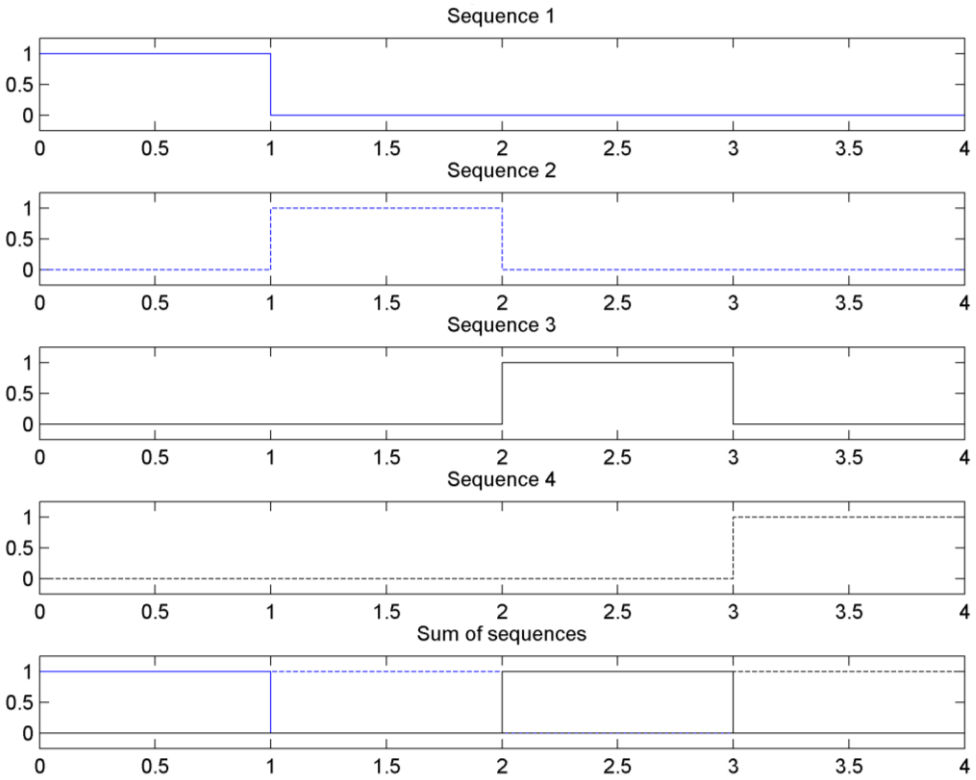

Figure 3.1. The set of length 4 PPCs shown individually, as well as with non-overlapping sum of sequences.

The cross-correlation between sequence 1 and sequence 3 in Fig. 3.1 is shown in Fig. 3.2. It should be observed that $\theta(\boldsymbol{c}_1, \boldsymbol{c}_3)(0) = 0$. This shows that the two sequences are orthogonal. The correlation peak seen at $\tau = -2$ is considered a side-lobe. Correlation side-lobes do not cause interference in synchronous transmission systems. However, in asynchronous transmission or time-dispersive channel conditions, a correlation side-lobe can shift to the zero shift position. This is known as MUI and results in a loss of orthogonality, resulting in interference between transmissions using different sequences. Therefore, an orthogonal signal set with zero side-lobe values would be required for transmission under asynchronous or time-dispersive conditions.

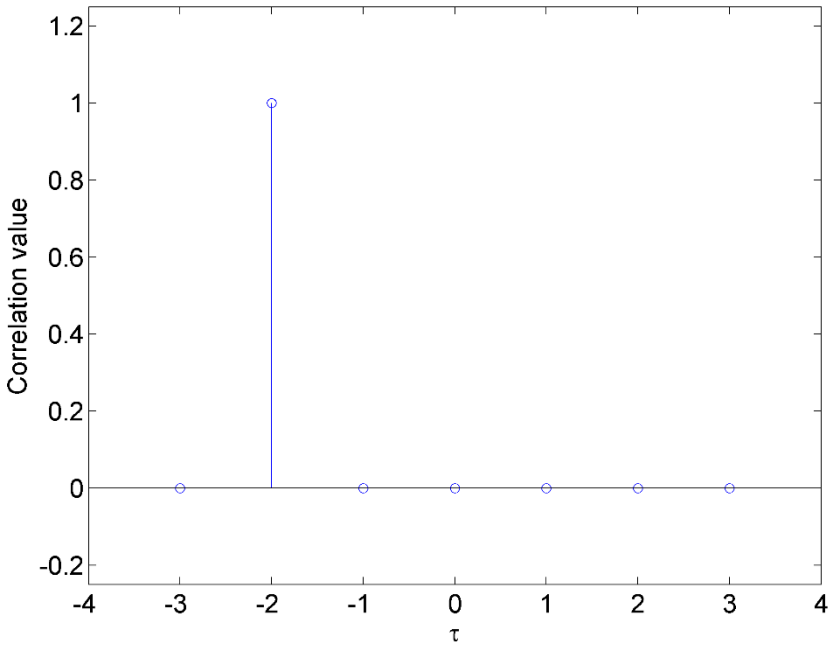

Figure 3.2. Cross-correlation between length 4 PPC sequence 1 and sequence 3.

3.2.1 Periodic correlation

Periodic correlation makes use of the convolution theorem of the FT which states that

$$x(t) * y(t) \leftrightarrow X(f) \cdot Y(f), \tag{3.2}$$

with $X(f)$ and $Y(f)$ the frequency domain transforms of $x(t)$ and $y(t)$ respectively. As correlation is mathematically equivalent to convolution with the time domain reversal of one sequence, the correlation can be performed in the frequency domain using multiplication. The result is then transformed back into the time domain to get the final correlation output. This is known as the cross-correlation theorem of the FT. For a discrete system, the periodic correlation between two signals, $\theta(x[n], y[n])[\tau]$, is given by

$$\theta(x[n_t], y[n_t])[\tau] = ifft(\left(X\left[n_f\right]\right)^* \cdot (Y\left[n_f\right])), \tag{3.3}$$

where $X[n_f]$ and $Y\left[n_f\right]$ are the frequency domain transforms of $x[n_t]$ and $y[n_t]$ respectively, and $(\square)^*$ denotes the transpose operator. The advantage of periodic

correlation is that all cyclic rotated versions of the original sequence will correlate with the original sequence at the correlator output corresponding to the shift between the sequences.

3.2.2 Signal space

As signals can be represented by vectors, several orthogonal vectors can be combined to create a signal space. The axes of the signal space are represented by base vectors, which are the vector representations of the base signals used to represent the signals.

Using the vector representation of the length 2 PPCs, it can be seen in Fig. 3.3 that the sequences can be shown as orthogonal vectors on a 2 dimensional plane. In this plane, the normalised version of the sequences are used as base vectors.

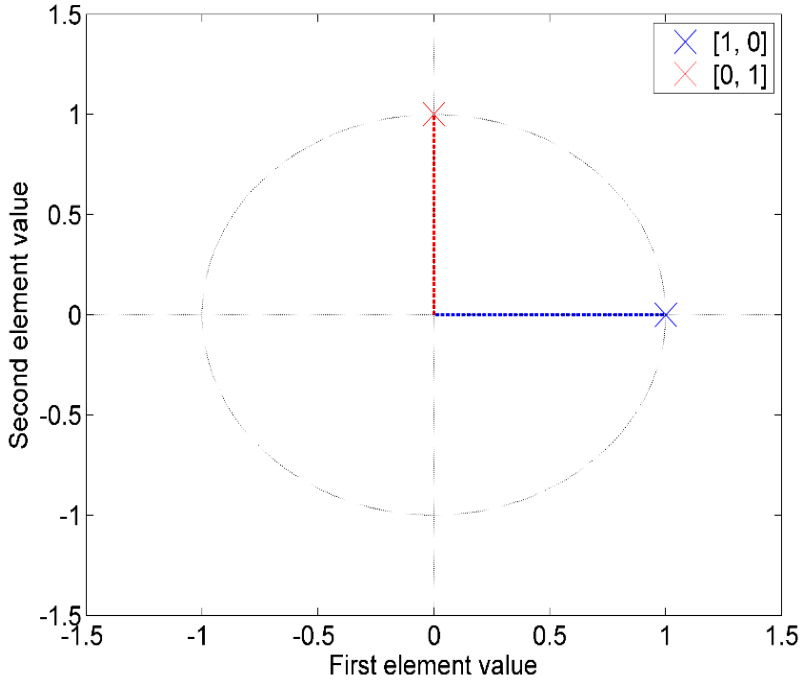

Figure 3.3. Vector representation of length 2 PPCs.

Another set of orthogonal sequences are the length 2 Walsh sequences:

$$\boldsymbol{c}_0 = [1, \quad 1]$$
$$\boldsymbol{c}_1 = [1, \quad -1].$$

It can be seen in Fig. 3.4 that these sequences can also be shown as being orthogonal on the same 2 dimensional plane as the PPCs.

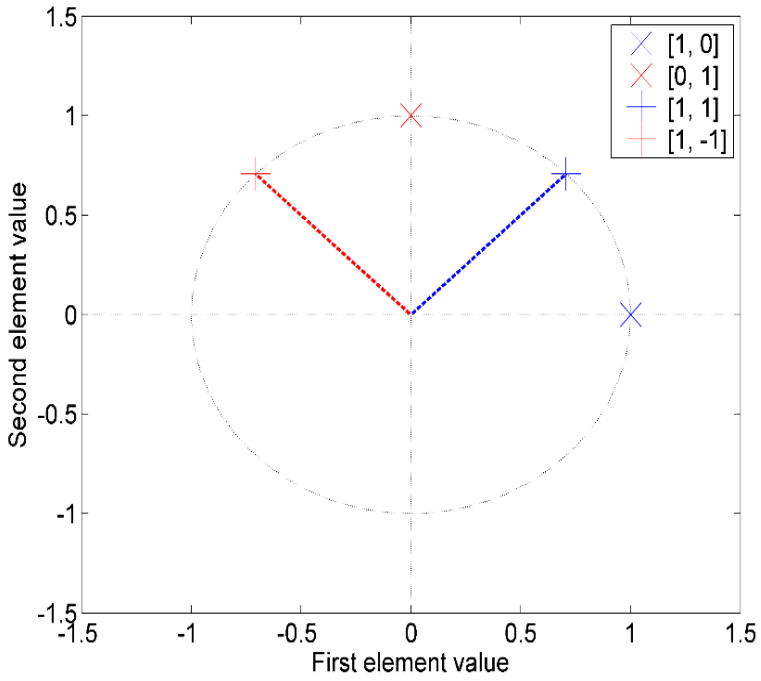

Figure 3.4. Vector representation of length 2 PPCs and Walsh sequences.

An amplitude scaling factor of $1/\sqrt{2}$ is used for the Walsh sequences in order to normalise the energy in each sequence to the same value of that for the PPCs, as the length 2 Walsh sequences have an energy of two times that of the PPCs.

Further, it can be seen that the 2 sets of sequences are in fact transformations of each other, by rotation of the sequence set about the origin. Orthogonality is maintained through rotation. This principle holds for higher dimensional systems as well, although it is difficult to represent higher dimensional signals in a two or three dimensional graph.

3.2.3 Multiple access

In telecommunication systems, it is often desirable to have several users share the same transmission spectrum. In order to ensure that the users do not interfere with each other, a technique has to be employed to provide users with non-interfering portions of the transmission resources. This is achieved through multiple access. Several multiple access schemes exists. Users can be allocated portions of the spectrum, different time slots, or

different access sequences. All multiple access schemes are based on orthogonal signals, in order to avoid interference with other users. This can be seen in Fig. 3.1 above, where each sequence can be seen as representing a different user.

3.3 POWER AMPLIFIERS

Radio frequency (RF) PAs are used in all radio transmission systems. PAs have non-linear power transfer characteristics near their maximum power output levels. An example is shown in Fig. 3.5.

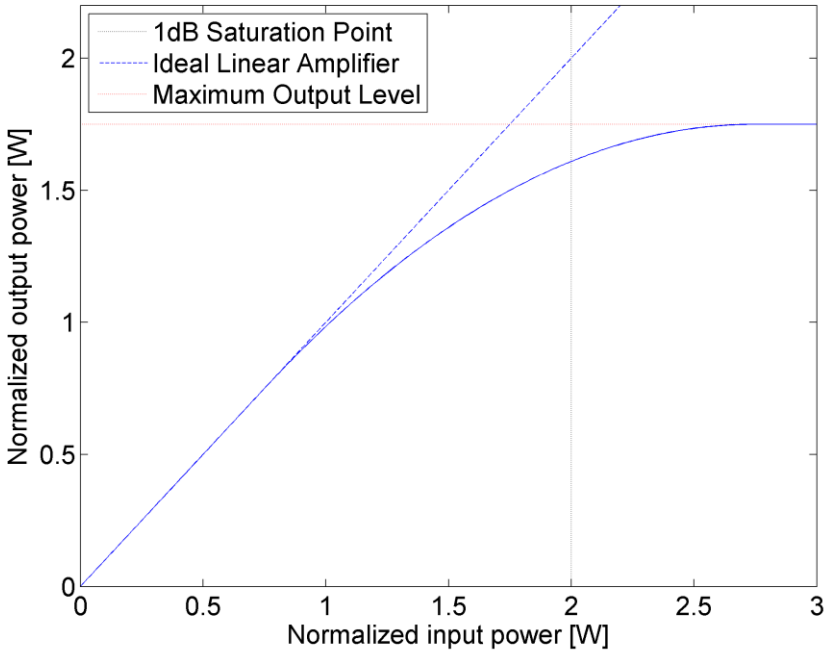

Figure 3.5. Power amplifier transfer characteristics.

These non-linear transfer characteristics lead to distortion of an amplified signal if the input signal drives the PA into saturation. Distortion of a signal can lead to the generation of out-of-band signal components that can cause interference with other systems. Examples of a PA distorting a signal is shown in Fig. 3.6 and Fig. 3.7 below. In Fig. 3.6 a signal is shown before and after amplification by a PA driven into soft saturation, i.e. distortion but not clipping the signal.

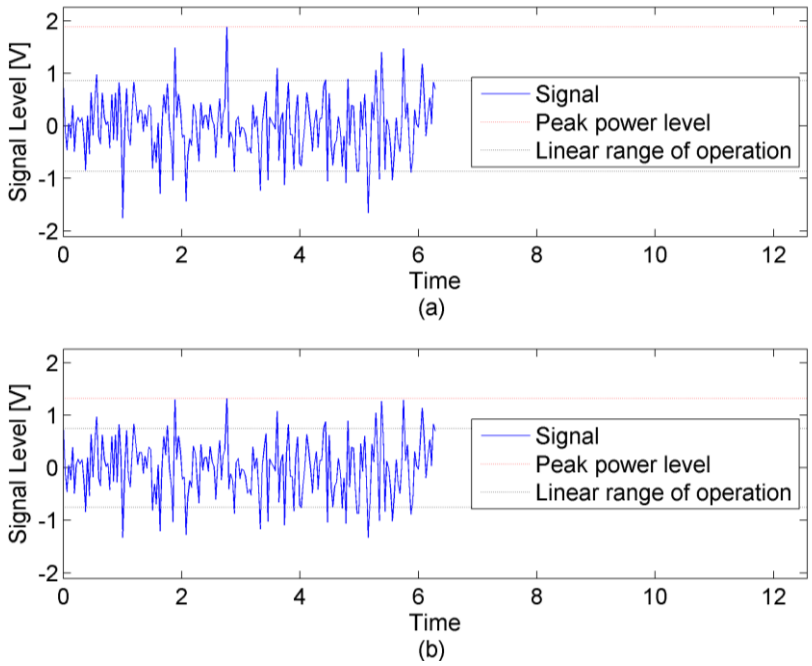

Figure 3.6. Non-linear distortion of amplified signal.

(a). Input signal. (b). Amplified signal.

From Fig. 3.6 it should be observed that the signal has become distorted due to the signal being outside the linear range of operation of the PA. In Fig. 3.7 the input and output power signals are shown, with relation to the amplifier power transfer curve. It should be observed that when input power peaks surpass the 1 dB saturation point of the amplifier, those peaks are amplified by a significantly reduced amount relative to the signal below the saturation point. This leads to distortion of the signal. Power peaks that surpass the peak power level of the amplifier are clipped to the peak power level.

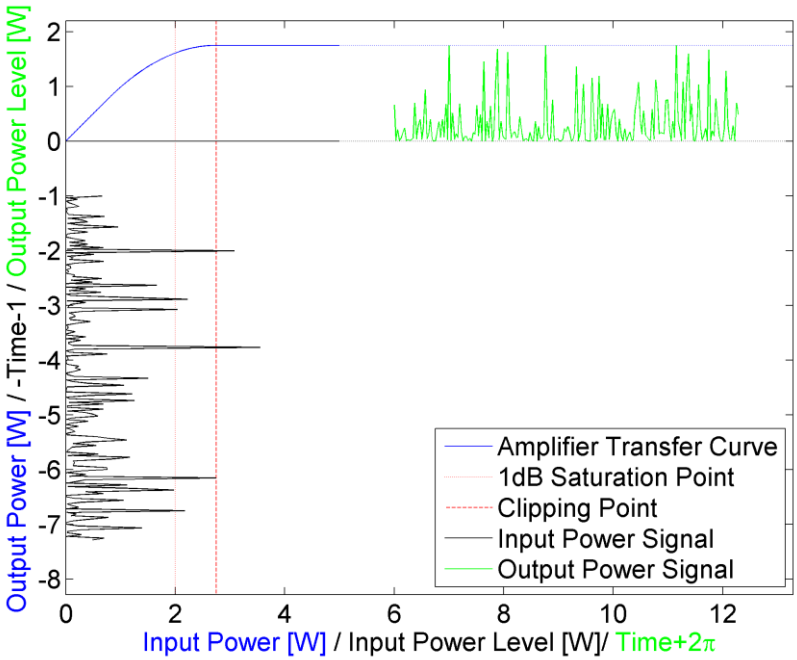

Figure 3.7. Input power signal (black) on power amplifier transfer curve (blue) with amplified power signal (green).

3.4 COMPLEMENTARY ROTATION KEYING

Complementary rotation keying (CRK) is a novel technique, which has been developed for this research. CRK is an orthogonal keying technique developed for improving the SE of CC-CDMA systems. The cyclic rotations of a flock of element sequences are used as the codewords for transmission. Only the cyclic rotations of the element sequences per flock are used for the transmission of the user associated with that flock. The number of bits of data per symbol $\boldsymbol{d}_v^{CRK}$ that can be modulated onto the choice of codeword per user is

$$k_{CRK} = log_2(L_E), \tag{3.4}$$

with L_E the element sequence length from (2.12). The rotation index, r, associated with the codeword to be transmitted is calculated through the binary to decimal conversion of the data $\boldsymbol{d}_v^{CRK}$,

$$r = bintodec(\boldsymbol{d}_v^{CRK}). \tag{3.5}$$

As $log_2(L_E) \ll L_E$ for large L_E, and the SE of a conventional CC-CDMA system is given by $1/L_E$, the system SE will decrease with increased L_E. As in CCSK, an additional modulation symbol, such as a BPSK or QPSK symbol, can be modulated onto the selected codeword to increase the SE, giving a bi-orthogonal or QPSK-CRK system, respectively.

The number of users that can be supported in CRK is the same as for a conventional CC-CDMA system, i.e. the number of flocks in the set $V = M$. This is an improvement over CCSK, where only one user can be supported. Most significantly, all the users in a CC-CDMA system do not have to use CRK. Users can be configured for either CRK or CR-CC-CDMA, depending on their SE and PAPR requirements, without causing MUI, due to the orthogonality of the flocks of sequences. This results in greater flexibility in system configuration.

3.5 CHAPTER OVERVIEW

The most important mathematical concepts used in this research have been described in order to provide a sufficient frame of reference for analysis of this research. The technique of CRK has been presented and will be analysed in detail in the following chapters. The possibility of combining CRK and CR-CC-CDMA into a joint CC-CDMA system has also been introduced.

CHAPTER 4 SYSTEM MODEL

4.1 CHAPTER OVERVIEW

Two different CC-CDMA configurations for improving the SE of low PAPR CC-CDMA sequences are investigated. The first configuration is based on CR-CC-CDMA, and is described in Section 4.2. The second configuration is based on CRK, and is presented in Section 4.3. It should be noted that these configurations are both based on the rotation of the element sequences of a CCC set. These configurations are therefore compatible to a large extent, and can be implemented within the same communication system.

4.2 CYCLIC ROTATION COMPLETE COMPLEMENTARY CODE DIVISION MULTIPLE ACCESS

The CR-CC-CDMA configuration is used to greatly improve the SE of a conventional CC-CDMA system. The amount of SE improvement is scalable, allowing for a possible trade-off between SE and PAPR performance. The system block diagram of the transmitter for CR-CC-CDMA is shown in Fig. 4.1.

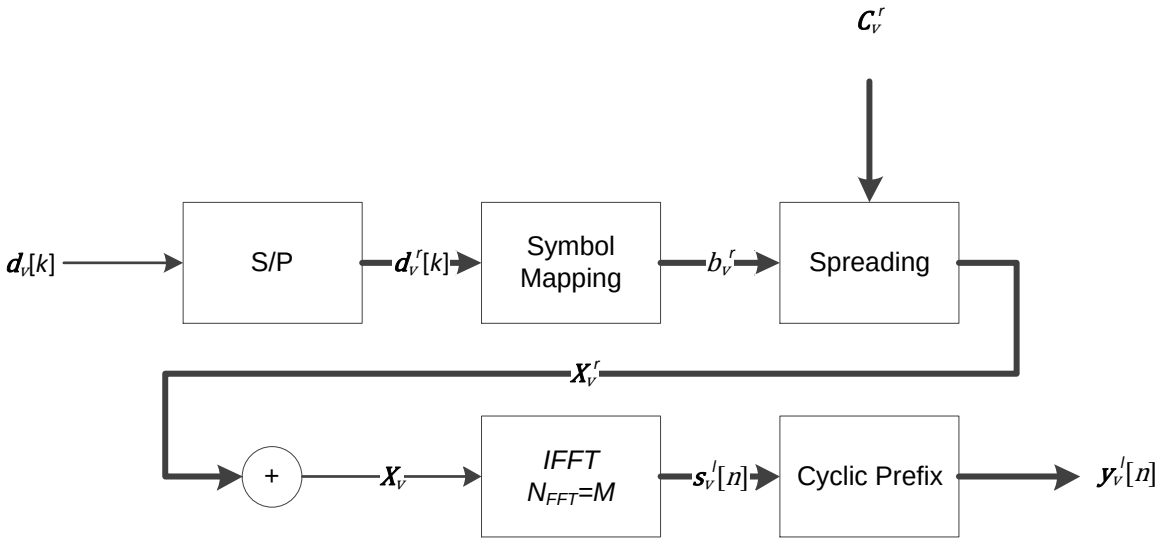

Figure 4.1. Transmitter structure for CR-CC-CDMA.

Firstly a series-to-parallel (S/P) converter is used in order to split the data stream $\boldsymbol{d_v}[k]$ into multiple data sub-streams, $\boldsymbol{d_v^r}[k]$, with $r \in [1, R], R \leq L_E$ with R the number of data

sub-streams used and L_E the number of columns in the spreading matrix $\boldsymbol{C_v}$. The maximum number of data sub-streams per flock is L_E, although fewer data sub-steams can be used in proportion to the SE requirements of the user. The number of bits per data sub-stream, k_v^r, need not be the same, although, unlike OFDM, each data sub-stream will experience the same channel conditions and therefore will not suffer from a reduced signal-to-noise ratio (SNR) relative to each other. Each data sub-stream is then mapped to modulation symbols b_v^r using conventional modulation symbols such as QPSK or M-QAM. Modulation symbols are spread using their assigned spreading matrix $\boldsymbol{C_v^r}$. This generates a spread matrix $\boldsymbol{X_v^r}$ for each data sub-stream. The spreading matrix for each data symbol is a cyclic rotated version of the original flock of sequences assigned to the user $\boldsymbol{C_v} = \boldsymbol{C_v^0}$. If all rotations are not used, rotations with maximum feasible separation are used, i.e.

$$r \in \left\{k \times \frac{L_E}{R}\right\}, k \in \{0, R-1\}, \tag{4.1}$$

where R is a power of 2, such that R equals or exceeds the number of rotations required for the desired SE. Unused rotations cannot be assigned to another user, unless the system is fully synchronous. During each time slot, all the rows from a column $l \in \{0, L_E - 1\}$ of all of the spread matrices are summed together. This is viable as the symbols will be orthogonal after combining at the receiver. The columns of the summation of the spread matrices are used as frequency domain symbols $\boldsymbol{X_v}$, with each row representing a different subcarrier. The different columns represent different time slots. A column-wise IFFT with $N_{FFT} = M$ is used to modulate the frequency domain symbols onto their respective subcarriers to create a time domain signal block $\boldsymbol{s_v^l}[n]$ per timeslot l. The sampling frequency of the IFFT is chosen based on the required BW. A CP is added to each time domain signal block to create a transmission time domain signal block $\boldsymbol{y_v^l}[n]$ with the CP length L_{CP} based on the expected channel conditions. After a transmission time domain signal block and its CP have been transmitted, the next column is modulated and transmitted. Once all columns of the spread matrix have been transmitted, new data to be transmitted are entered into the S/P converter. The system block diagram of the receiver for CR-CC-CDMA is shown in Fig. 4.2.

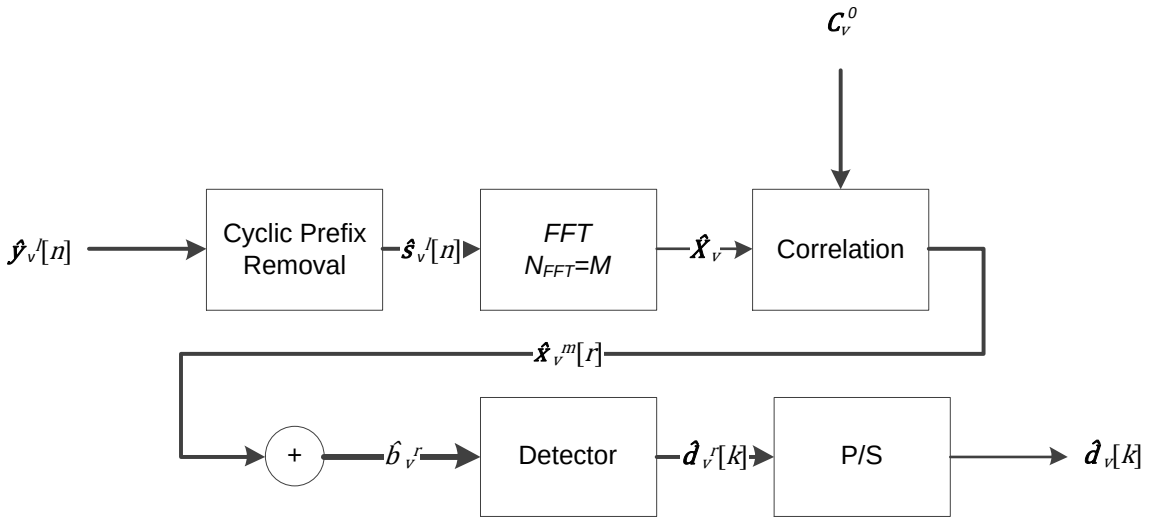

Figure 4.2. Receiver structure for CR-CC-CDMA.

At the receiver the received signal $\hat{\boldsymbol{y}}_v^l[n]$ is firstly read into a memory element of length $N_{FFT} + L_{CP}$. This procedure is performed in order to remove the CP from the received signal, creating a received time domain signal block $\hat{\boldsymbol{s}}_v^l[n]$ per timeslot l. During each timeslot the received signal block is demodulated using an FFT of length $N_{FFT} = M$, as in the transmitter. The output of the FFT are the recovered frequency domain symbols $\hat{\boldsymbol{X}}_v$. The recovered frequency domain symbols are stored into a second memory element of size $L_E \times M$. After all timeslots associated with a spread matrix have been received and the memory element filled, correlation is performed on the recovered frequency domain symbols using the flock of spreading sequences $\boldsymbol{C_v} = \boldsymbol{C_v^0}$ assigned to the user. Periodic correlation is used as only one operator is required to recover all the transmitted modulation symbols. Each row of the recovered frequency domain symbols are correlated individually as is required in CC-CDMA. After correlation, the correlator outputs $\hat{\boldsymbol{x}}_v^m[r]$ are summed together. The summation output is the recovered modulation symbol for each data sub-stream $\hat{b}_v^r$, scaled by the PG. The element position of the summation output corresponds to the rotation index r used for each data symbol. The recovered modulation symbols are then de-mapped using a conventional detector for the type of modulation used in the transmitter. The outputs of the detector are the recovered data sub-streams $\hat{\boldsymbol{d}}_v^r[k]$.

The recovered data sub-streams are combined into the recovered data stream $\widehat{\boldsymbol{d}}_v[k]$ through a parallel to series (P/S) converter.

4.3 QUADRATURE PHASE SHIFT KEYING COMPLEMENATARY ROTATION KEYING

The QPSK-CRK configuration is used to improve the SE of a conventional CC-CDMA system, while maintaining its PAPR properties. When a CC-CDMA system is implemented using the QPSK-CRK configuration and a low PAPR CCC, the PAPR of the QPSK-CRK configuration will be limited to the PAPR of the low PAPR CC-CDMA sequences, i.e. 3 dB. The system block diagram of the transmitter for QPSK-CRK is shown in Fig. 4.3.

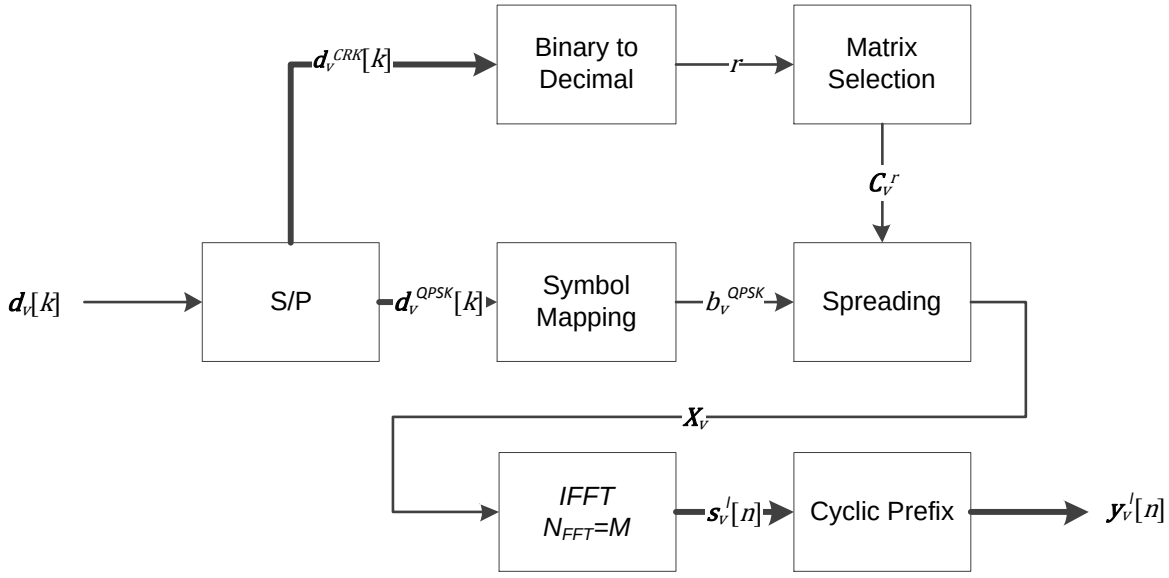

Figure 4.3. Transmitter structure for QPSK-CRK.

Firstly, a S/P converter is used in order to split the data stream $\boldsymbol{d}_v[k]$ into 2 data sub-streams, $\boldsymbol{d}_v^{QPSK}[k]$ and $\boldsymbol{d}_v^{CRK}[k]$. The $\boldsymbol{d}_v^{QPSK}[k]$ data sub-stream consists of 2 bits and is mapped to a QPSK modulation symbol b_v^{QPSK}. The $\boldsymbol{d}_v^{CRK}[k]$ data sub-stream is used to

determine which spreading matrix $\boldsymbol{C}_v^r$ is used to spread the data symbol. This is calculated through binary to decimal conversion

$$r = bintodec(\boldsymbol{d}_v^{CRK}[k]). \tag{4.2}$$

The number of bits k_{CRK} in $\boldsymbol{d}_v^{CRK}[k]$ is dependent on the length of the element sequences L_E in the spreading matrix $\boldsymbol{C_v}$, from (3.4). Once a spreading matrix is chosen based on (4.2), the QPSK modulation symbol b_v^{QPSK} is spread to create a spread matrix $\boldsymbol{X}_v$. The columns of the spread matrix are used as frequency domain symbols, with each row representing a different subcarrier. The different columns represent different timeslots. A column-wise IFFT with $N_{FFT} = M$ is used to modulate the frequency domain symbols onto their respective subcarriers to create a time domain signal block $\boldsymbol{s}_v^l[n]$ per timeslot l. The sampling frequency of the IFFT is chosen based on the required BW. A CP is added to each time domain signal block to create a transmission time domain signal $\boldsymbol{y}_v^l[n]$ with the CP length L_{CP} based on the expected channel conditions. After a time domain signal block and its CP have been transmitted, the next column is modulated and transmitted. Once all columns of the spread matrix have been transmitted, new data to be transmitted are entered into the S/P converter. The system block diagram of the receiver for QPSK-CRK is shown in Fig. 4.4.

The recovered frequency domain symbols are stored into a second memory element of size $M \times L_E$. After all time slots associated with a spread matrix have been received and the memory element filled, correlation is performed on the recovered frequency domain symbols using the flock of spreading sequences $\boldsymbol{C_v} = \boldsymbol{C_v^0}$ assigned to the user. Periodic correlation is used as only one operator is required to calculate all the correlator outputs. Each row of the recovered frequency domain symbols are correlated individually as is required in CC-CDMA. After correlation, the correlator outputs $\hat{\boldsymbol{x}}_v^m[r]$ are summed together. The outputs of the summation $\hat{b}_v^r$ are sent to a decision device to estimate which spreading matrix index $\hat{r}$ was used. The summation output at position $\hat{r}$ is the recovered modulation symbol $\hat{b}_v^{QPSK}$ and is then de-mapped using a QPSK detector.

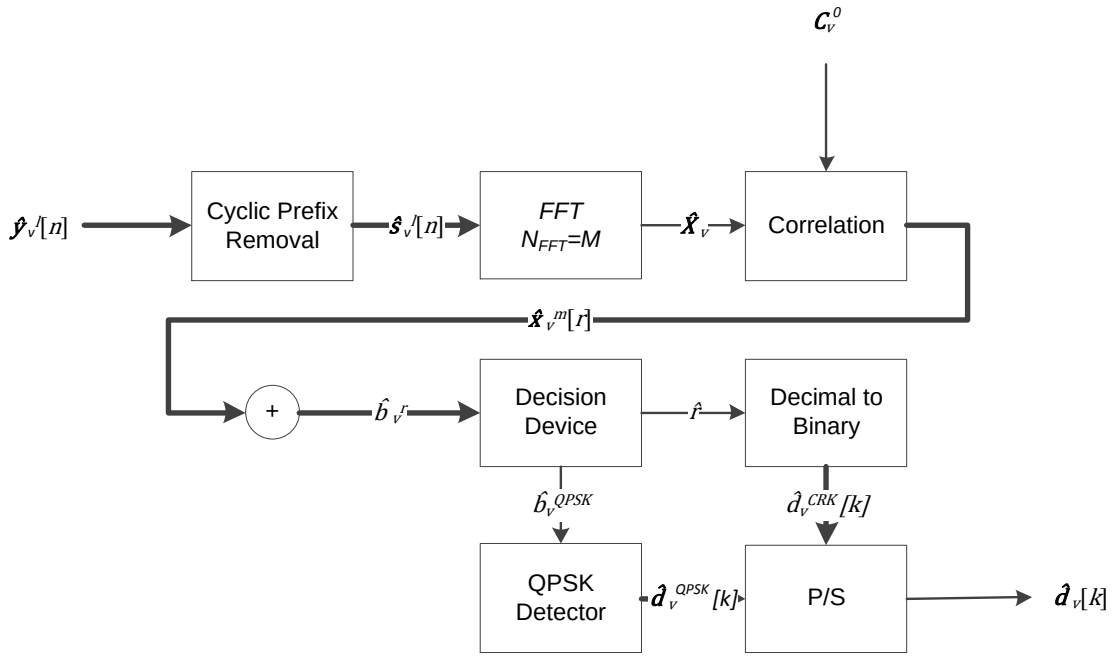

Figure 4.4. Receiver structure for QPSK-CRK.

The output of the detector is the recovered data sub-stream $\widehat{\boldsymbol{d}}_v^{QPSK}$ and the decimal to binary conversion of $\hat{r}$ is the recovered position data sub-stream $\widehat{\boldsymbol{d}}_v^{CRK}$. The recovered sub-streams $\widehat{\boldsymbol{d}}_v^{QPSK}[k]$ and $\widehat{\boldsymbol{d}}_v^{CRK}[k]$ are combined into the recovered data stream $\widehat{\boldsymbol{d}}_v[k]$ using a P/S converter.

4.4 CHAPTER OVERVIEW

The functional system models of CR-CC-CDMA and CRK have been described in this chapter. It has been shown that the models share a majority of their functional blocks. This indicated that the techniques might be implemented in a joint system without significant complexity increase. The simulation models of the presented models are described in the following chapter.

CHAPTER 5 SIMULATION MODELS

5.1 CHAPTER OVERVIEW

A simulation model of the transmitter and receiver for the CR-CC-CDMA and QPSK-CRK configurations has been developed. As CR-CC-CDMA and QPSK-CRK are interoperable, a single transmitter and receiver structure was developed that can be configured for either configuration with minimal adjustment. The CCCs used in this research are listed in Section 5.2. The PAPR simulation model is described in Section 5.3. The BER simulation model is presented in Section 5.4.

5.2 CODES USED

Three sets of CCCs were used for simulation:

i) The first CCC is a low PAPR CCC from [13] (Example 3) and is shown in Appendix A. For the first CCC that was used, $L_E = 32, V = M = 8, q = 4$.

ii) The second CCC from [13] (Example 2), is not a low PAPR CCC, and was only used for BER simulation and comparison.

iii) A third CCC was generated based on the method of [13] and used for comparative BER results. Parameters for the third CCC are $L_E = 64, V = M = 64, q = 2$. Theorem 3 from [13] and the GBFs of

$$f(\boldsymbol{x}) = \boldsymbol{x_0x_5 + x_1x_5 + x_2x_5 + x_3x_5 + x_4x_5 + x_0x_1 + x_1x_2 + x_3x_4}$$
$$h(\boldsymbol{y}) = \boldsymbol{y_0y_1 + y_1y_2 + y_2y_3 + y_3y_4 + y_4y_5}$$

with $J = \{0,1,2,3,4\}$, $J' = \{5\}$, $W = \{0,1,2,3,4\}$, $\{w_k\} = \{5\}$, with W' an empty set, were used. The value of $M = 64$ was chosen as this results in $N_{FFT} = 64$, similar to some modern MC systems, such as IEEE 802.11n [6].

5.3 PEAK-TO-AVERAGE POWER RATIO SIMULATION MODEL

For simulation of the PAPR of the CR-CC-CDMA and QPSK-CRK configurations, only the transmitters, shown in Fig. 4.1 and Fig.4.3, are considered. A block of transmitter symbols is generated from random data, and the PAPR of the block is computed. The transmitter symbols are generated using QPSK modulation symbols for both CR-CC-CDMA and QPSK-CRK. The PAPR is calculated in decibels. This is done for

each user individually. The number of transmitter symbols per block was set to 10. The number of blocks was set to 10^4. This value was chosen to ensure accurate results at 10^{-2} probability on the complementary cumulative distribution function (CCDF) of the PAPR. The PAPR values were collected for each block. After all blocks have been evaluated, the CCDF of the PAPR is determined. The PAPR of several OFDM configurations are used for comparison. The CCDFs are presented on a logarithmic scale. A simulation of ACE implemented on CR-CC-CDMA was performed in order to determine if additional PAPR reduction could be achieved. For the ACE transmitter, $PAPR_{THR} = 4$ dB, $P_{CLP} = 4$ dB were used. ACE was chosen as it is the preferred technique for PAPR reduction in OFDM systems. The PAPR of DFT-s OFDM is known from literature, and is only included for reference.

5.4 BIT ERROR RATE SIMULATION MODEL

For the simulations of the BER of the CR-CC-CDMA and QPSK-CRK configurations, both the transmitter (Fig. 4.1 and Fig. 4.3) and receiver (Fig. 4.2 and Fig. 4.4) are considered. The BER performance for CR-CC-CDMA is known from existing literature [10]. BER performance results for CR-CC-CDMA presented in this research are only included to confirm correct performance of the simulation model. A block of transmitter symbols is generated from random data. The transmitter symbols are generated using QPSK modulation symbols for both CR-CC-CDMA and QPSK-CRK. AWGN is added to the transmitter symbols to simulate the effect of a noisy channel, before being processed by the receiver in order to recover the transmitter data. The data are then compared to the transmitter data to calculate the BER. The AWGN is generated as a complex Gaussian distributed complex random vector with unit variance for each user v. The variance of each user's noise vector is scaled by a scaling factor ${\varepsilon_n}^v$ in order to evaluate the system performance at different SNR values. For CR-CC-CDMA the scaling factor is calculated as

$${\varepsilon_n}^v = \sqrt{\frac{N_0}{2*E_b} * L_e}, \tag{5.1}$$

and for QPSK-CRK

$$\varepsilon_n{}^v = \sqrt{\frac{N_0}{E_b} * L_e * \left(\frac{1}{2 + \log_2 L_e}\right)}, \tag{5.2}$$

where N_0 is the single sided noise spectral density, E_b is the average energy per bit, L_E is the length of the element sequence as in (2.12). This is repeated for each user individually. Fading channel models are not simulated as the system does not utilize an optimal receiver for mitigating the phase ambiguity introduced in fading channels. The receiver can be configured to simulate a single user or multi-user system. The number of transmitted symbols per block was set to 1. The number of blocks was set based on the number of bits per user, in order to achieve an accurate result at 10^{-4} BER probability for the CR-CC-CDMA configuration. As the BER for QPSK-CRK is significantly lower than a BPSK system in AWGN, the number of blocks was set in order to achieve an accurate result at 10^{-3} BER probability. The effects of an asynchronous user is investigated in the joint system configuration. This is done by delaying the transmitted signal of a single user by an integer chip offset.

5.5 CHAPTER OVERVIEW

The simulation models for CR-CC-CDMA and QPSK-CRK, as well as the CCCs used in this research have been presented in this chapter. These models and CCCs are used to generate the results shown in the following chapter. The example CCC from [13] is used to provide results comparable to that available in existing literature.

CHAPTER 6 RESULTS

6.1 CHAPTER OVERVIEW

In Section 6.2 the PAPR results of both the CR-CC-CDMA and QPSK-CRK configurations as well as a joint system are presented, along with the PAPR performance of several state of the art systems for comparison. In Section 6.3 the BER results of both the CR-CC-CDMA and QPSK-CRK configurations in separate as well as a joint systems are presented.

6.2 PEAK-TO-AVERAGE POWER RATIO RESULTS

The PAPR results of the CC-CDMA system with both configurations are presented in this section.

6.2.1 Cyclic rotation complete complementary code division multiple access system

The PAPR performance of a CC-CDMA system using the CR-CC-CDMA configuration and the length 32 low PAPR CCC for a single user for different numbers of rotations is shown in Fig. 6.1. PAPR curves for two different OFDM configurations are also included for comparison. The first OFDM block size ($N_{FFT} = 8$) is based on the column size of the low PAPR CCC (M). The second OFDM block size ($N_{FFT} = 256$) is based on total SF ($L \times M$). The OFDM systems are fully loaded, as would be the case in an OFDM system that uses TDMA for multiple access. This will result in each user experiencing the PAPR of a fully loaded OFDM system during their assigned timeslot. It should be observed that the PAPR of the CR-CC-CDMA configuration using the length 32 low PAPR CCC varies based on the number of rotations used. For 2 or 4 rotations used, the system maintains a PAPR of 6 dB. For higher numbers of rotations, the PAPR increases while remaining between 1 and 1.5 dB below the PAPR of a fully loaded OFDM system with $N_{FFT} = 256$.

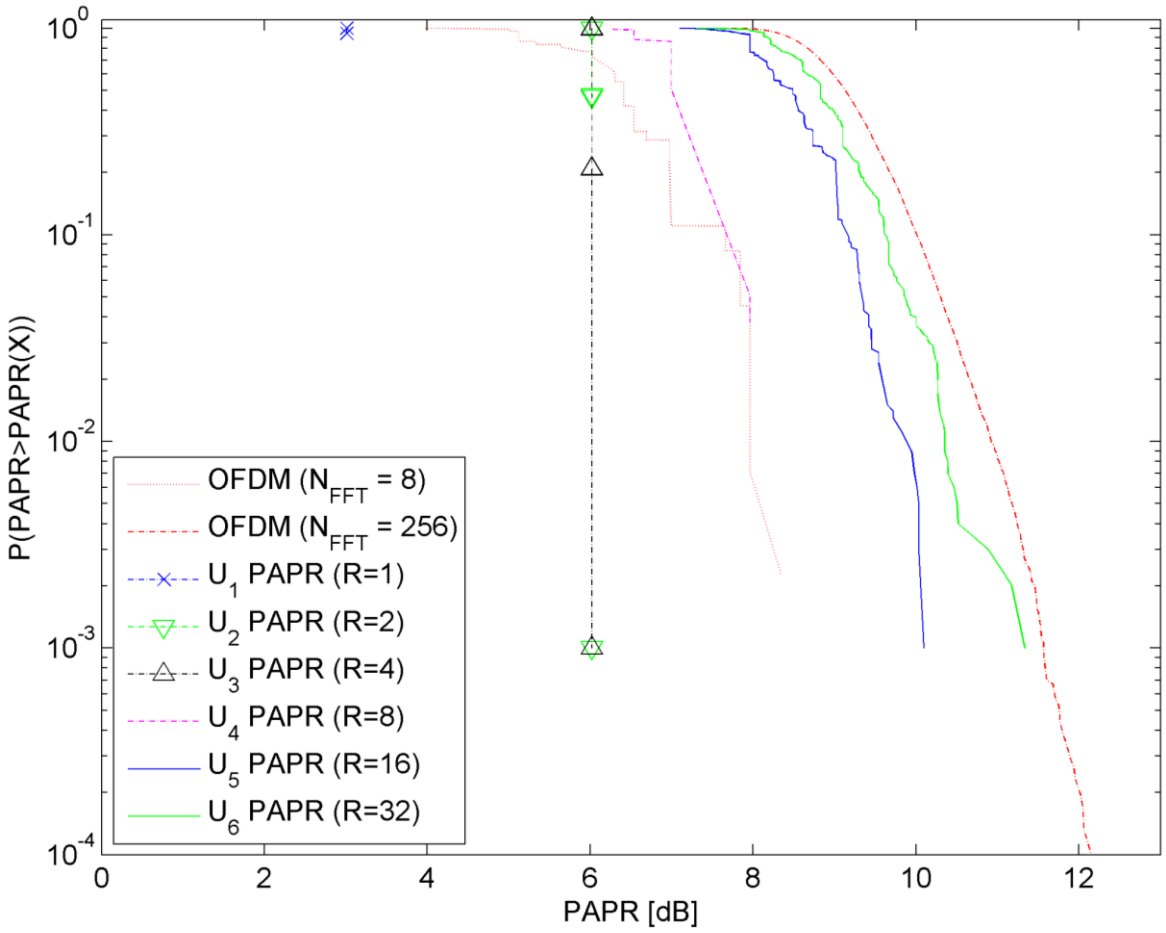

Figure 6.1. PAPR performance of CR-CC-CDMA with different number of rotations (R). It should be noted that $\boldsymbol{U_1}$ has a PAPR of 3 dB, and $\boldsymbol{U_2}$ and $\boldsymbol{U_3}$ has a PAPR of 6 dB.

A comparison of PAPR performance between a CC-CDMA system using the CR-CC-CDMA configuration and the length 32 low PAPR CCC and a conventional a CCC for different numbers of rotations used, is shown in Fig. 6.2. Users 1 through 4 are using the length 32 low PAPR CCC and users 5 through 8 are using the conventional CCC. It should be observed that the low PAPR CCCs offer a PAPR performance improvement for CR-CC-CDMA of between 1 and 3.5 dB at 10^{-2} probability.

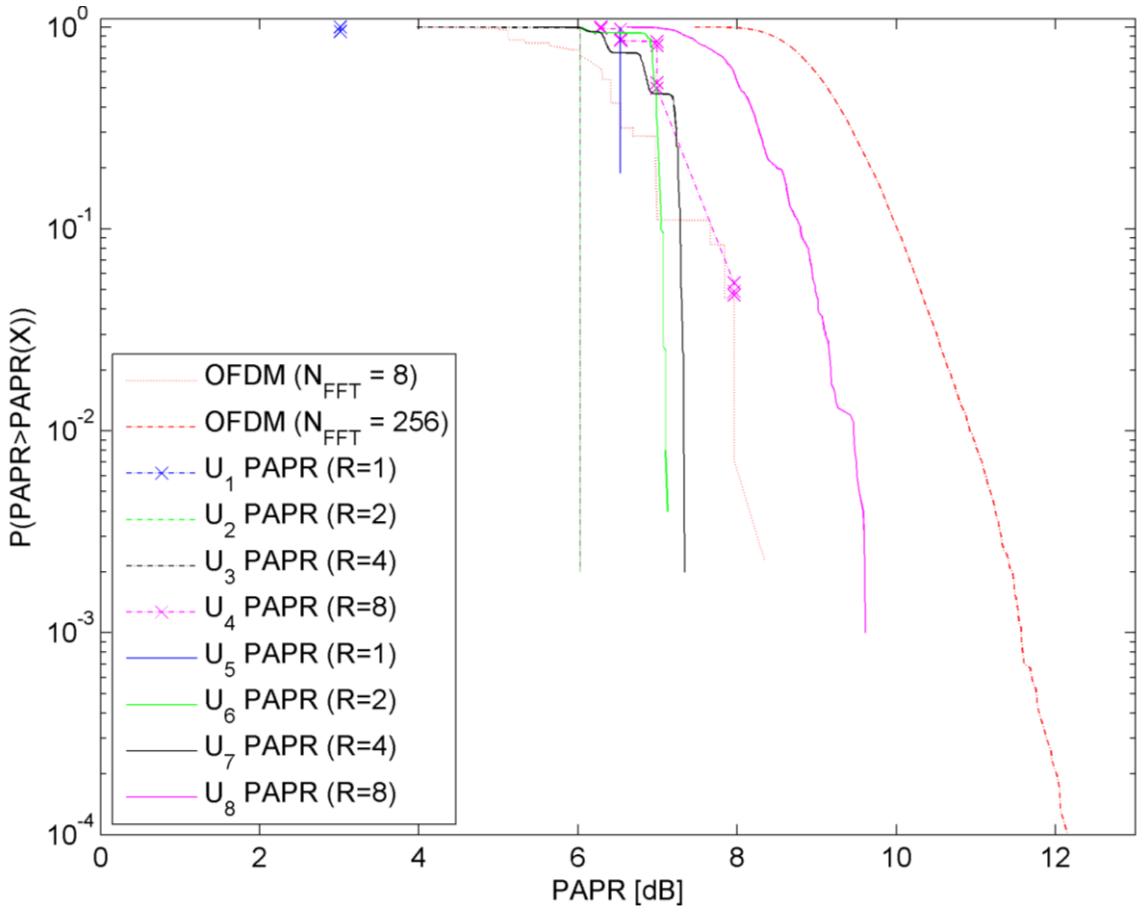

Figure 6.2. PAPR performance comparison between CR-CC-CDMA with low PAPR CCC and conventional CCC for low number of rotations (R). It should be noted that $\boldsymbol{U_1}$ has a PAPR of 3 dB, and $\boldsymbol{U_2}$ and $\boldsymbol{U_3}$ both have a PAPR of 6 dB.

A comparison of the PAPR between a CC-CDMA system using the CR-CC-CDMA configuration and the length 32 low PAPR CCC with and without ACE is shown in Fig. 6.3. The reference curves for OFDM and the CR-CC-CDMA systems are different to Fig. 6.1 and Fig. 6.2. This is due to the PAPR for ACE being measured per symbol, not over several symbols. It should be observed that the implementation with ACE does improve the PAPR of the CR-CC-CDMA configuration by between 0.5 and 1 dB at 10^{-2} probability. The increase in performance is proportional to the number of rotations used.

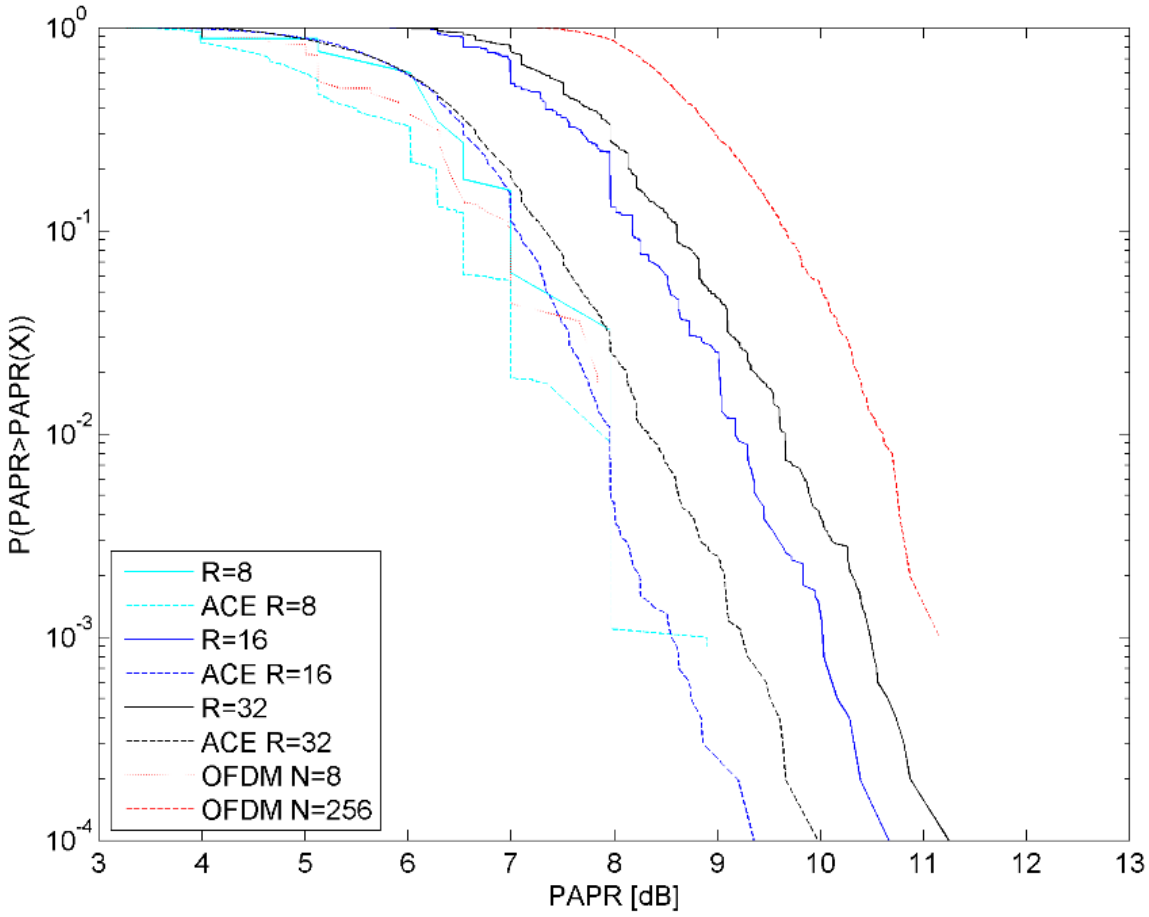

Figure 6.3. PAPR performance comparison of CR-CC-CDMA with and without ACE for high number of rotations (R).

6.2.2 Quadrature phase shift keying complementary rotation keying

The PAPR performance of a CC-CDMA system using the QPSK-CRK configuration and the length 32 low PAPR CCC is shown in Fig. 6.4. The zero rotations ($R = 0$) assigned to each user, indicated that the user is configured for QPSK-CRK. It should be observed that the PAPR of the QPSK-CRK configuration remains at 3 dB for all users.

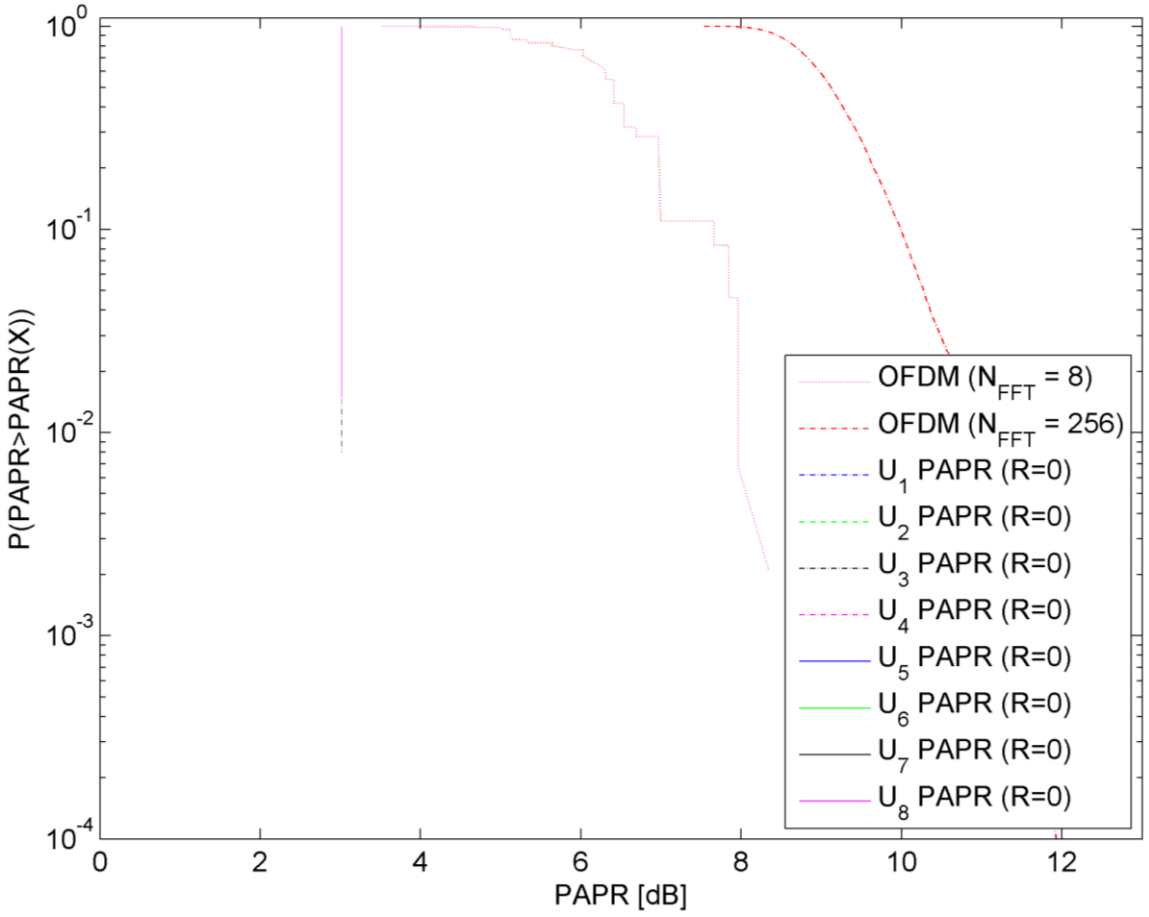

Figure 6.4. PAPR performance of QPSK-CRK. The curves for all users are present at 3 dB. R=0 indicating the use of QPSK-CRK.

6.2.3 Joint system performance

The PAPR performance of a CC-CDMA system using the length 32 low PAPR CCC is shown in Fig. 6.5. In this system, users are randomly assigned a different number of rotations. The zero rotations ($R = 0$) assigned to user 7, indicates that this user is configured for QPSK-CRK, while all other users are configured for CR-CC-CDMA. It should be observed that the QPSK-CRK configuration has the same PAPR of 3 dB as the CR-CC-CDMA configuration with $R = 1$, and a better PAPR than $R = 2$ or $R = 4$. For $R > 4$, the CR-CC-CDMA configuration has a PAPR that increases in proportion to the number of rotations used.

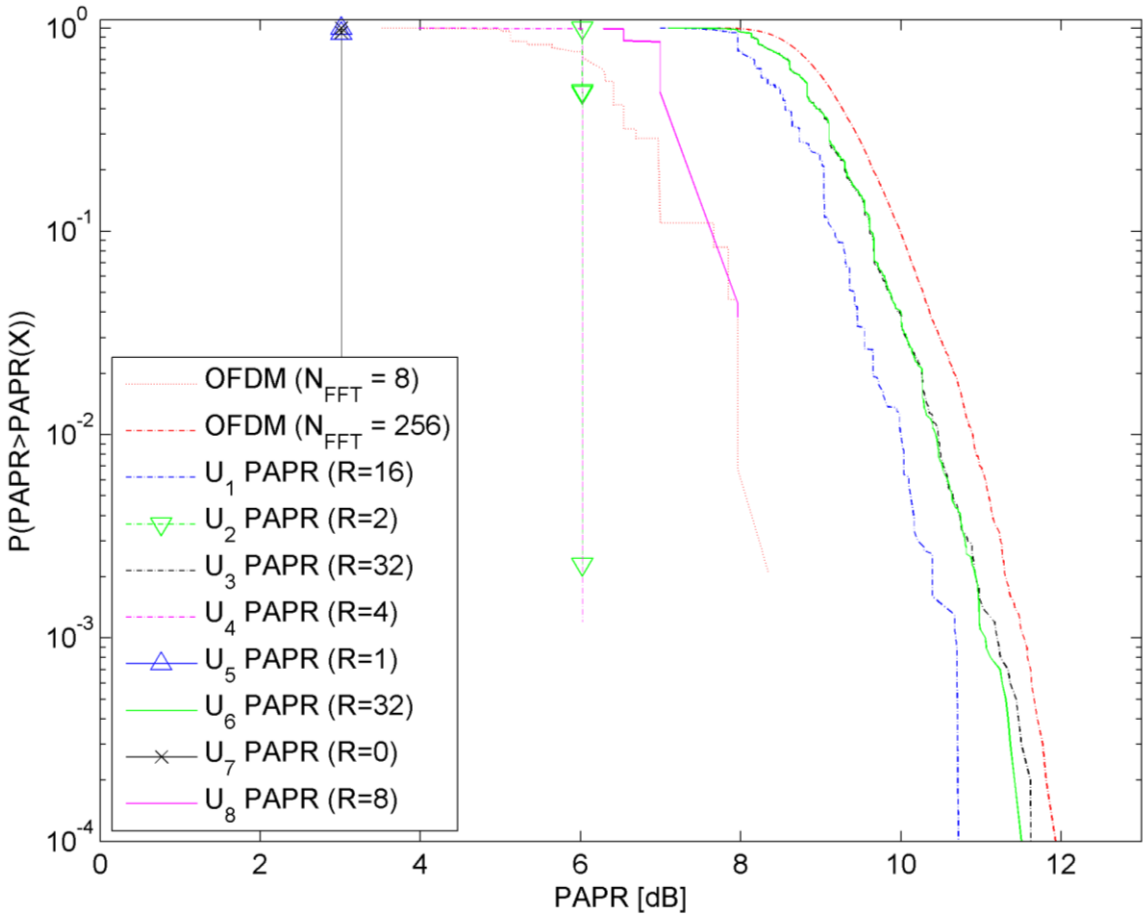

Figure 6.5. PAPR performance of CR-CC-CDMA with randomly selected number of rotations per user (R) and QPSK-CRK (R=0) in a joint system. It should be noted that $\boldsymbol{U_5}$ and $\boldsymbol{U_7}$ have a PAPR of 3 dB and $\boldsymbol{U_2}$ and $\boldsymbol{U_4}$ have a PAPR of 6 dB.

6.2.4 Discrete Fourier transform spread orthogonal frequency division multiplexing system

A comparison of the PAPR of OFDMA and DFT-s OFDM systems with different FFT lengths is shown in Fig. 6.6. All systems are partially loaded to $1/8$ of their maximum throughput, in order to be comparable to the results of the length 32 CCC (not shown in Fig. 6.6). The DFT-s OFDM is using a localized configuration, as is used in LTE.

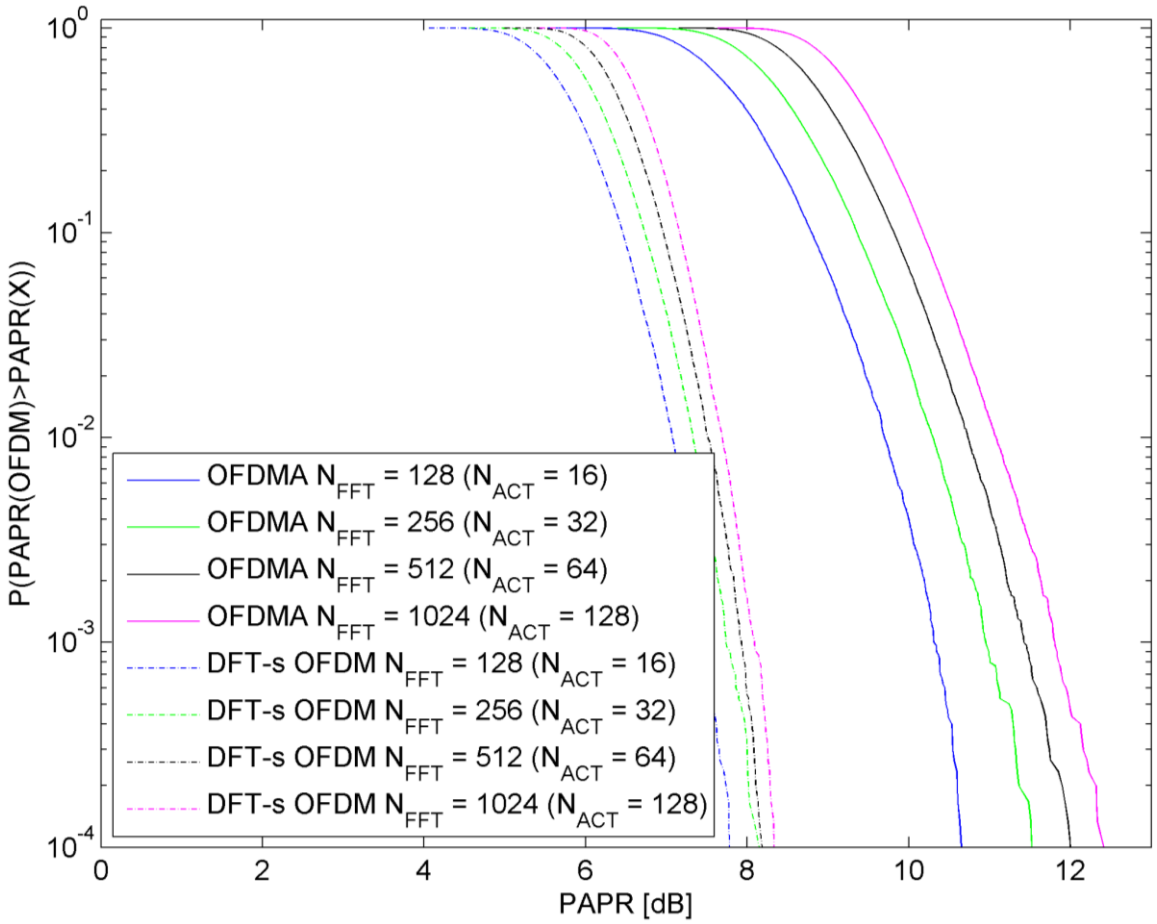

Figure 6.6. PAPR performance of DFT-s OFDM compared to partially loaded OFDMA. N_{ACT} the number of utilised subcarriers.

It should be observed that the PAPR of each of the DFT-s OFDM systems is lower than the corresponding OFDMA system by between 2 and 3 dB at 10^{-2} probability. The difference in PAPR for all configurations of DFT-s OFDM is less than 1 dB. The minimum PAPR at 10^{-2} probability is 7 dB.

6.3 BIT ERROR RATE RESULTS

The BER results of the CC-CDMA system with both configurations are presented in this section.

6.3.1 Cyclic rotation complete complementary code division multiple access system

BER performance for CR-CC-CDMA is known from existing literature [10]. BER performance results presented in this sub-section are only included to confirm proper performance of the simulation model. The single user BER performance of a CC-CDMA system using the CR-CC-CDMA configuration and the length 32 low PAPR CCC in AWGN is shown in Fig. 6.7 for different numbers of rotations. It should be observed that, for all numbers of rotations, the BER performance of the CR-CC-CDMA configuration remains on the theoretical curve for BPSK in AWGN.

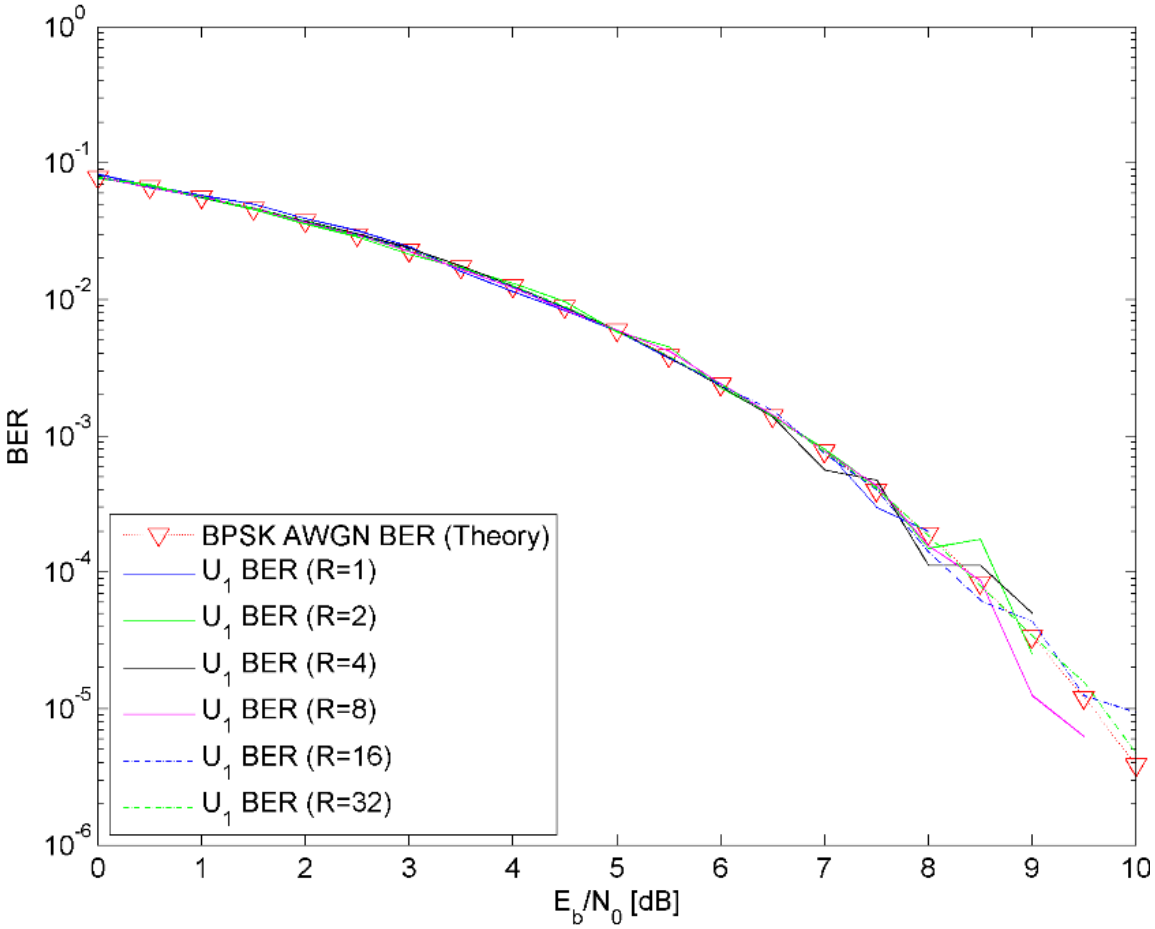

Figure 6.7. Single user BER performance of CR-CC-CDMA in AWGN for different numbers of rotations (R). BER curves for all rotations lay on the same line.

The multiuser BER performance of a CC-CDMA system using the CR-CC-CDMA configuration and the length 32 low PAPR CCC for all users with the maximum number of

rotations for each user in AWGN is shown in Fig. 6.8. It should be observed that the BER performance of the CR-CC-CDMA configuration remains on the theoretical curve for BPSK in AWGN for all users.

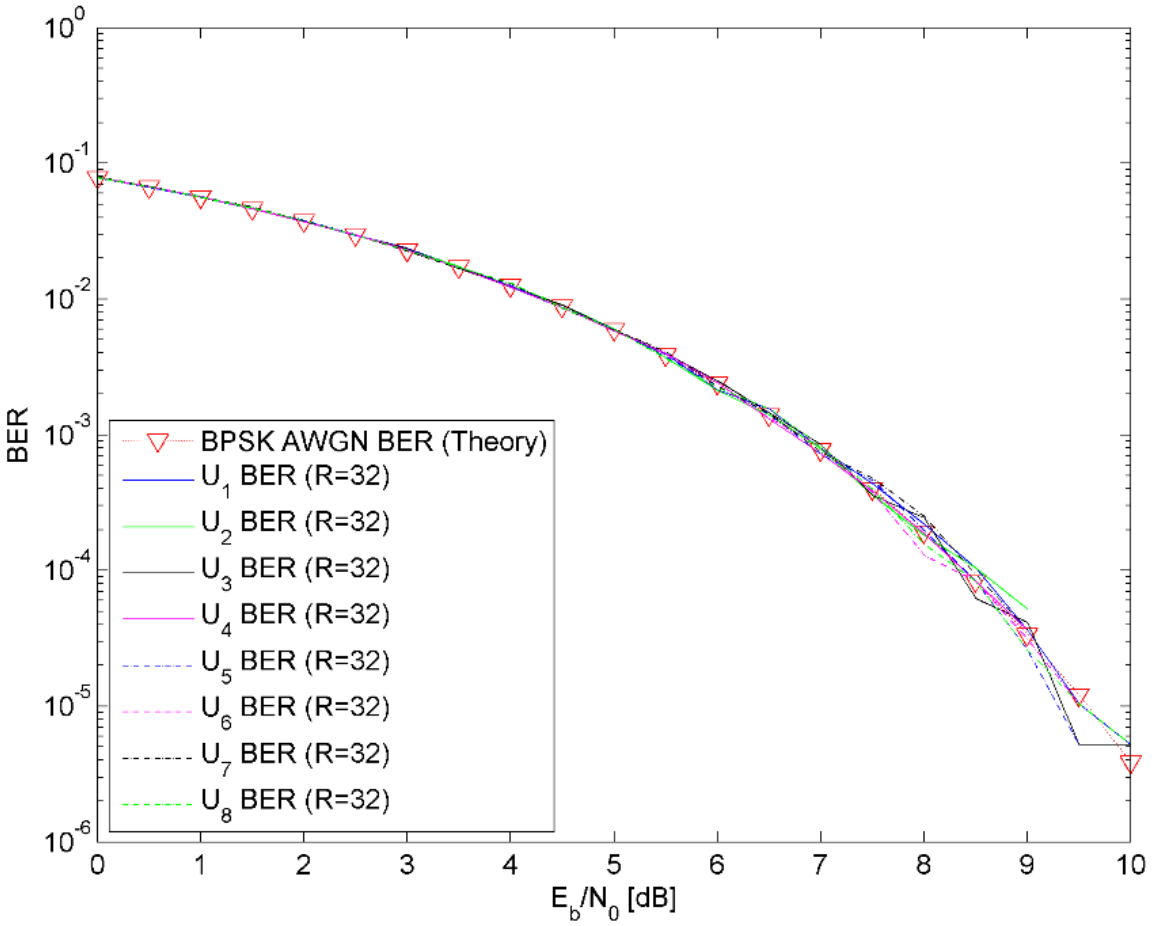

Figure 6.8. Multi-user BER performance of CR-CC-CDMA in AWGN for maximum numbers of rotations (R). BER curves for all users lay on the same line.

For comparison, the multiuser BER performance of a CC-CDMA system using the CR-CC-CDMA configuration and the length 64 low PAPR CCC for a random set of users, with the maximum number of rotations for all users in AWGN is shown in Fig. 6.9. It should be observed that the BER performance of the CR-CC-CDMA configuration remains on the theoretical curve for BPSK in AWGN for all users.

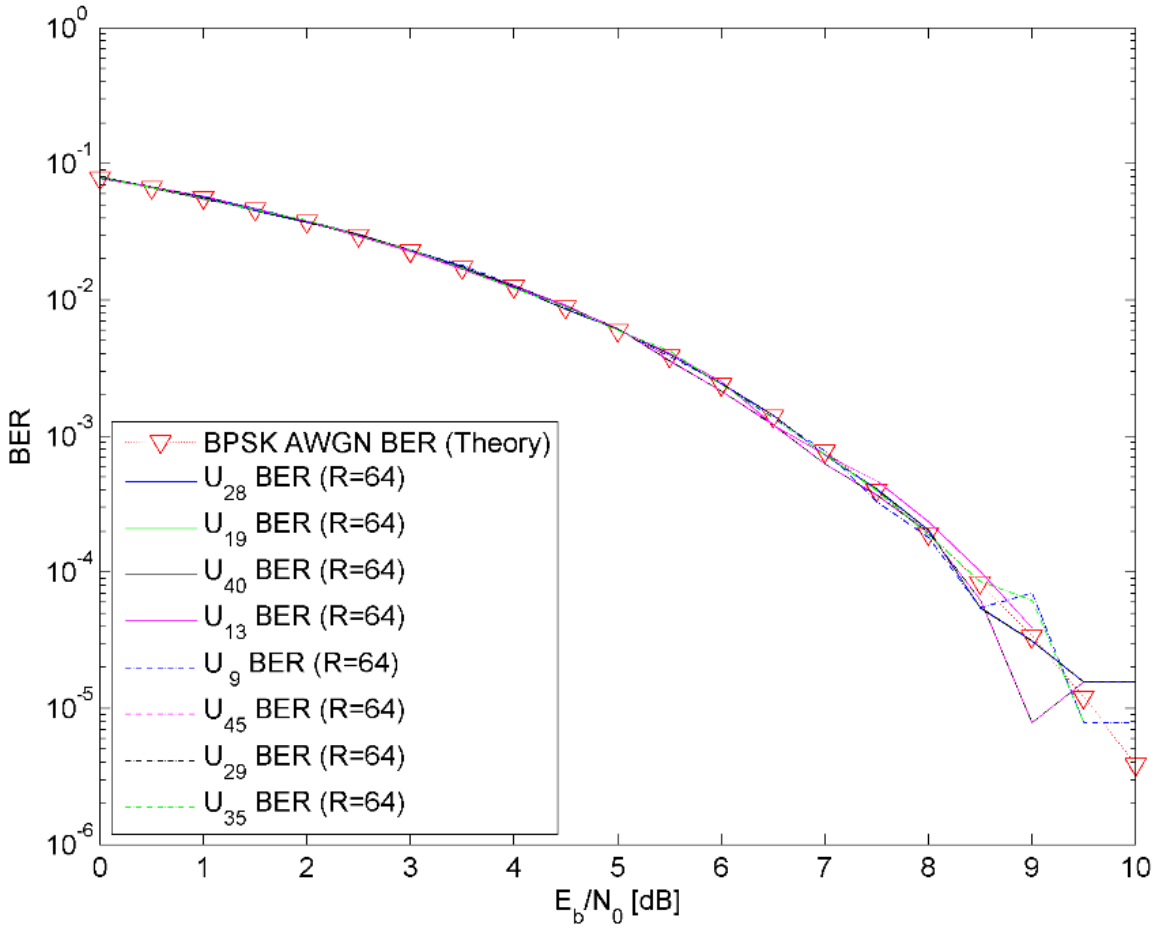

Figure 6.9. Multi-user BER performance of CR-CC-CDMA in AWGN for maximum number of rotations (R). BER curves for all users lay on the same line.

6.3.2 Quadrature phase shift keying complementary rotation keying

The single user BER performance of two CC-CDMA systems using the QPSK-CRK configuration and CCCs with different element sequence lengths in AWGN is shown in Fig. 6.10. It should be observed that the BER performance of QPSK-CRK is approximately 2 to 3 dB better than BPSK in AWGN at 10^{-3} BER probability. The BER performance of the QPSK-CRK configuration is approximately 1 dB better than the corresponding upper bounds for M-FSK. Both BER curves closely follow the upper bounds for M-FSK with $M = L_E * 4$. Additionally, it should be observed that the BER decreases as the element sequence length is increased.

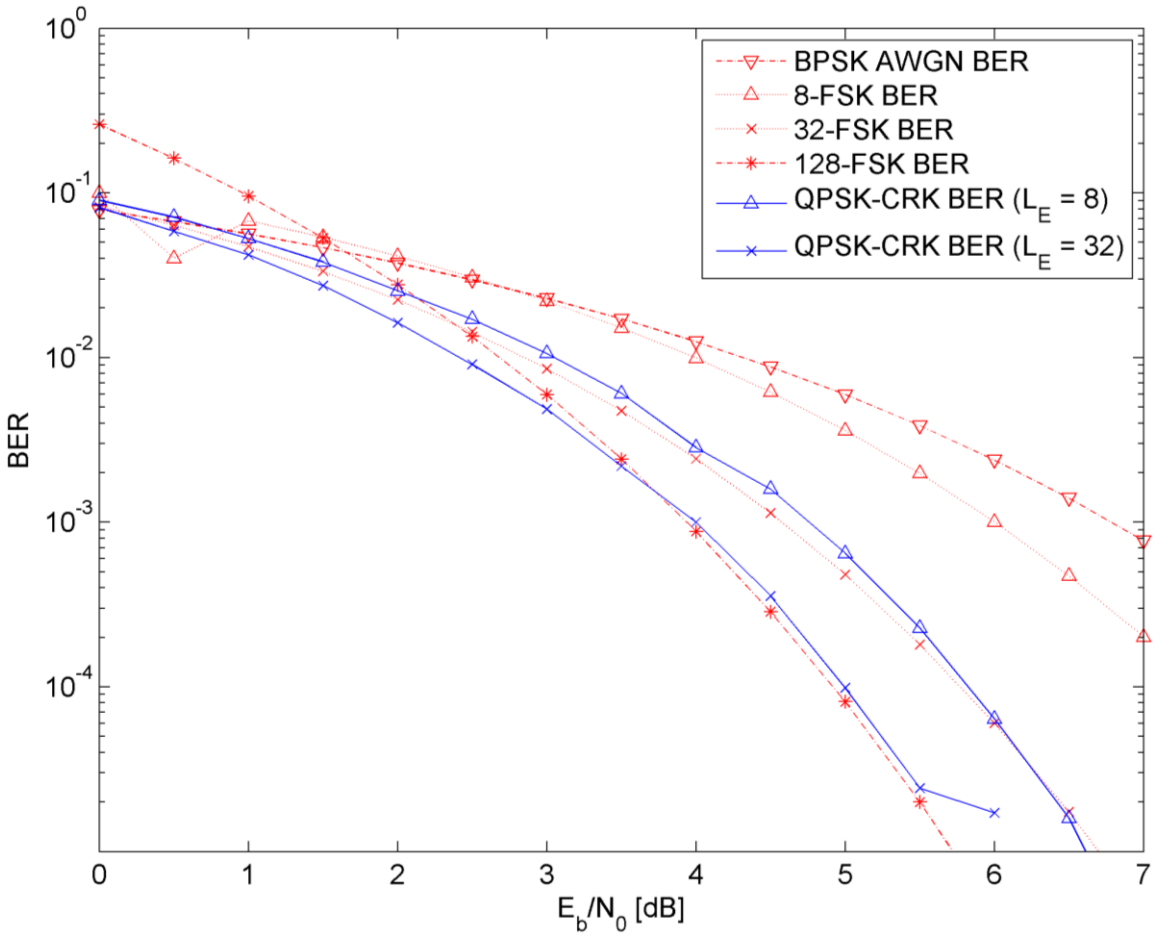

Figure 6.10. Single user BER performance of QPSK-CRK in AWGN for different element sequence lengths.

The multiuser BER performance of a CC-CDMA system using the QPSK-CRK configuration the length 32 low PAPR CCC for all users in AWGN is shown in Fig. 6.11. It should be observed that the BER performance of the QPSK-CRK configuration is 3 dB better than the theoretical curve for BPSK in AWGN at 10^{-3} BER probability, and approximately 1 dB better than 32-FSK for all users.

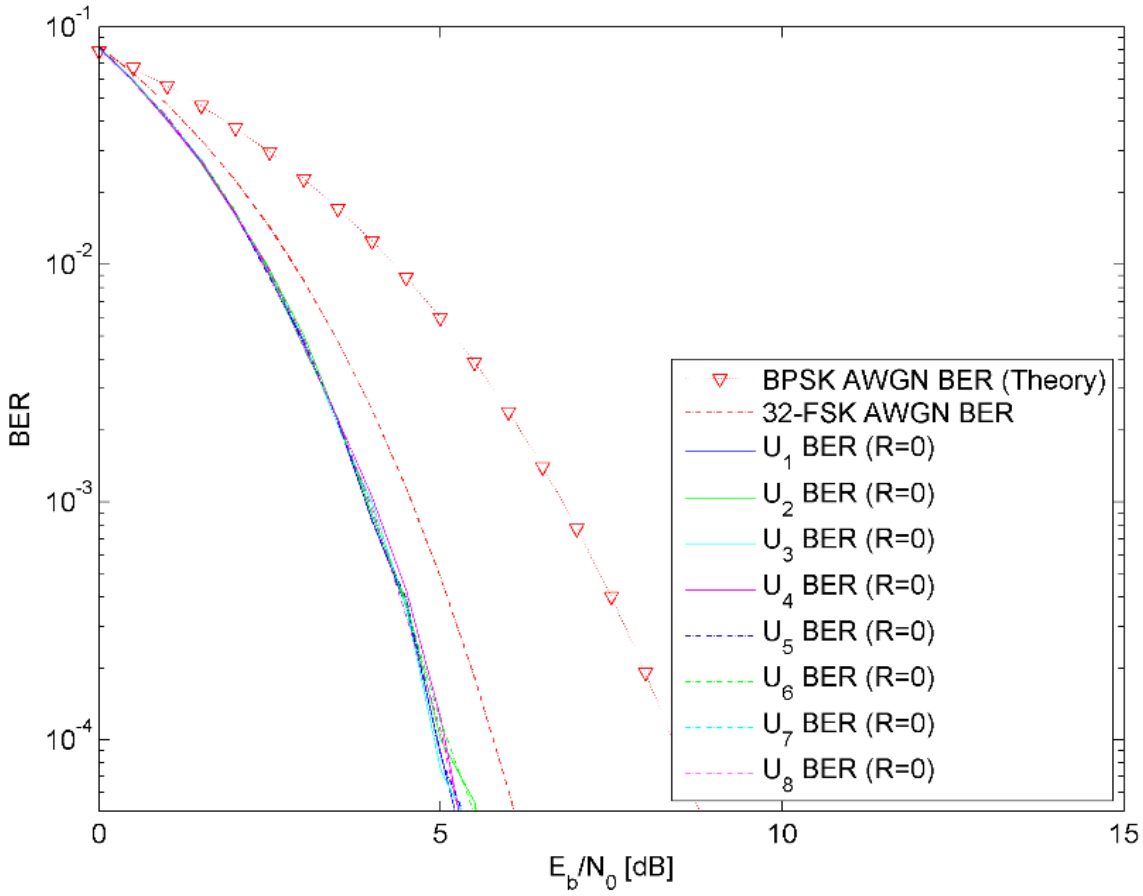

Figure 6.11. Multi-user BER performance of QPSK-CRK in AWGN. BER curves for all users lay on the same line. R=0 indicating the use of QPSK-CRK.

6.3.3 Joint system performance

The multiuser BER performance of a CC-CDMA system using the length 32 low PAPR CCC in AWGN is shown in Fig. 6.12. In this system, users are randomly assigned a different number of rotations. The 0 rotations ($R = 0$) assigned to user 7, indicates that this user is using QPSK-CRK, while all other users are using CR-CC-CDMA with the indicated number of rotations per user. It should be observed that the BER performance of both configurations remain unaffected in a joint system in AWGN for all users. The BER performance of users configured for CR-CC-CDMA remains on the theoretical curve for BPSK in AWGN. The BER performance of the user configured for QPSK-CRK is 3 dB

better than the theoretical curve for BPSK in AWGN and approximately 1 dB better than 32-FSK at 10^{-3} BER probability.

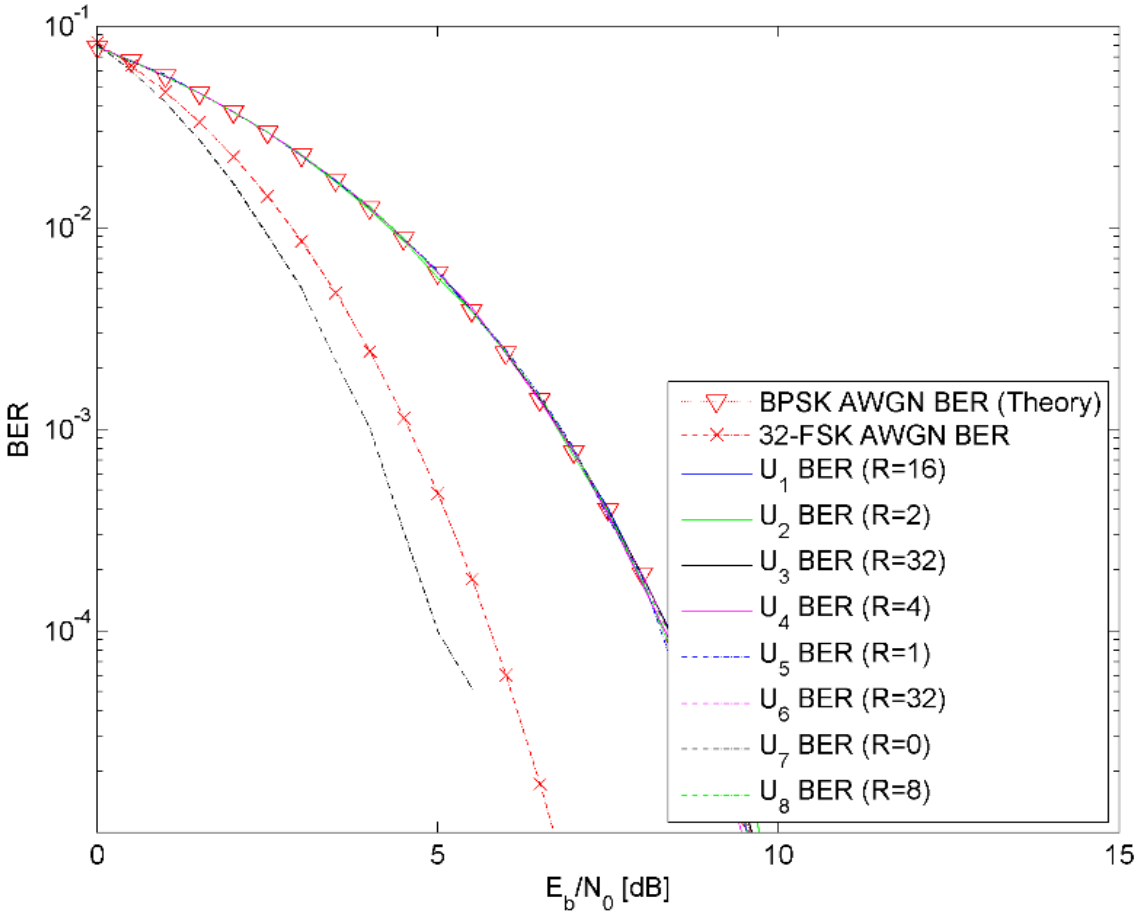

Figure 6.12. Multi-user BER performance of CR-CC-CDMA with randomly selected number of rotations per user (R) and QPSK-CRK (R=0) in a joint system in AWGN. BER curves for all CR-CC-CDMA users lay on the same line.

For comparison, the multiuser BER performance of a CC-CDMA system using the length 64 low PAPR CCC in AWGN is shown in Fig. 6.13. It should be observed that the BER performance of both configurations remain unaffected in a joint system in AWGN for all users. The BER performance of users configured for CR-CC-CDMA remains on the theoretical curve for BPSK in AWGN. The BER performance of the user configured for QPSK-CRK is 3.5 dB better than the theoretical curve for BPSK in AWGN and approximately 1 dB better than 32-FSK at 10^{-3} BER probability.

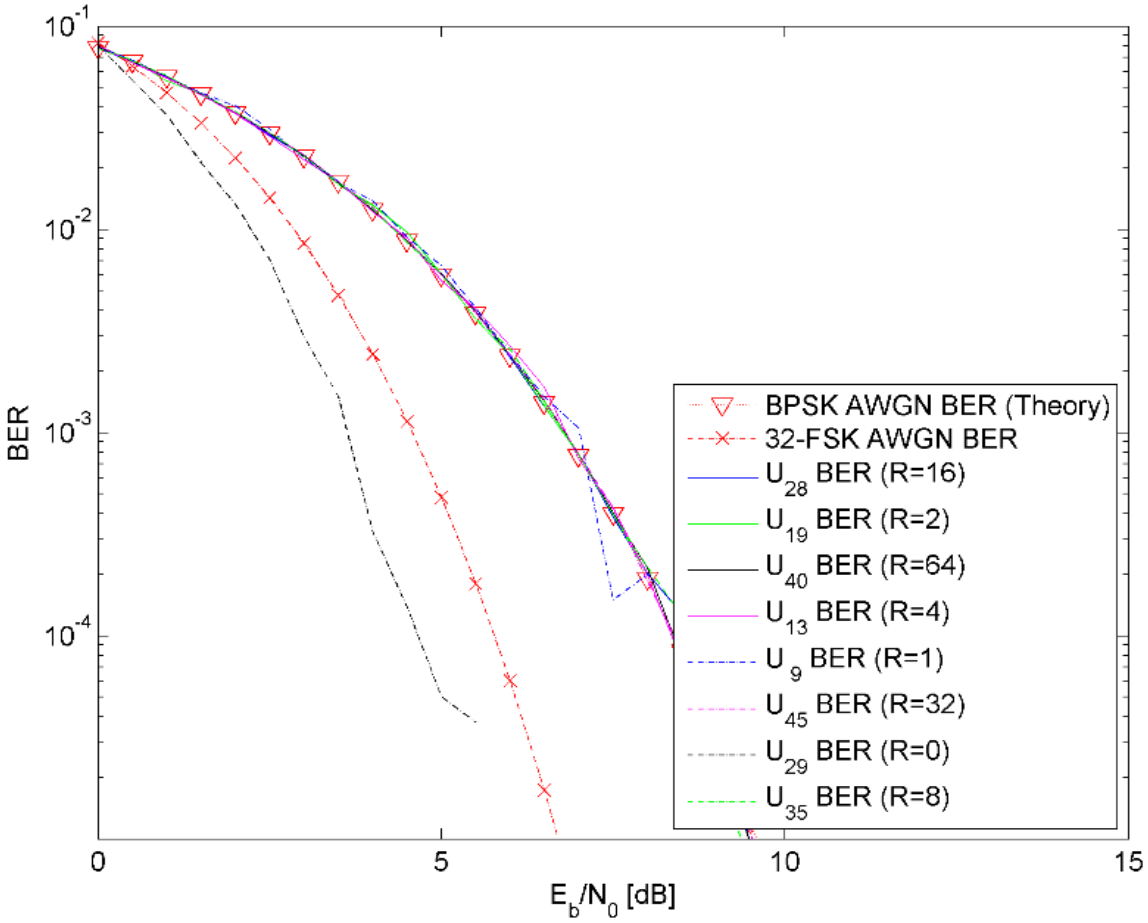

Figure 6.13. Multi-user BER performance of CR-CC-CDMA with randomly selected number of rotations per user (R) and QPSK-CRK (R=0) in a joint system in AWGN. BER curves for all CR-CC-CDMA users lay on the same line. Note BER reduction for U_{29} when compared to Fig. 6.12.

The multiuser BER performance of a CC-CDMA system using the length 32 low PAPR CCC with one asynchronous user in AWGN is shown in Fig. 6.14. It should be observed that the BER performance of both configurations remain unaffected, in a joint system with an asynchronous user in AWGN, for all users. The BER performance of users configured for CR-CC-CDMA remains on the theoretical curve for BPSK in AWGN. The BER performance of the user configured for QPSK-CRK is 3 dB better than the theoretical curve for BPSK in AWGN and approximately 1 dB better than 32-FSK at 10^{-3} BER probability.

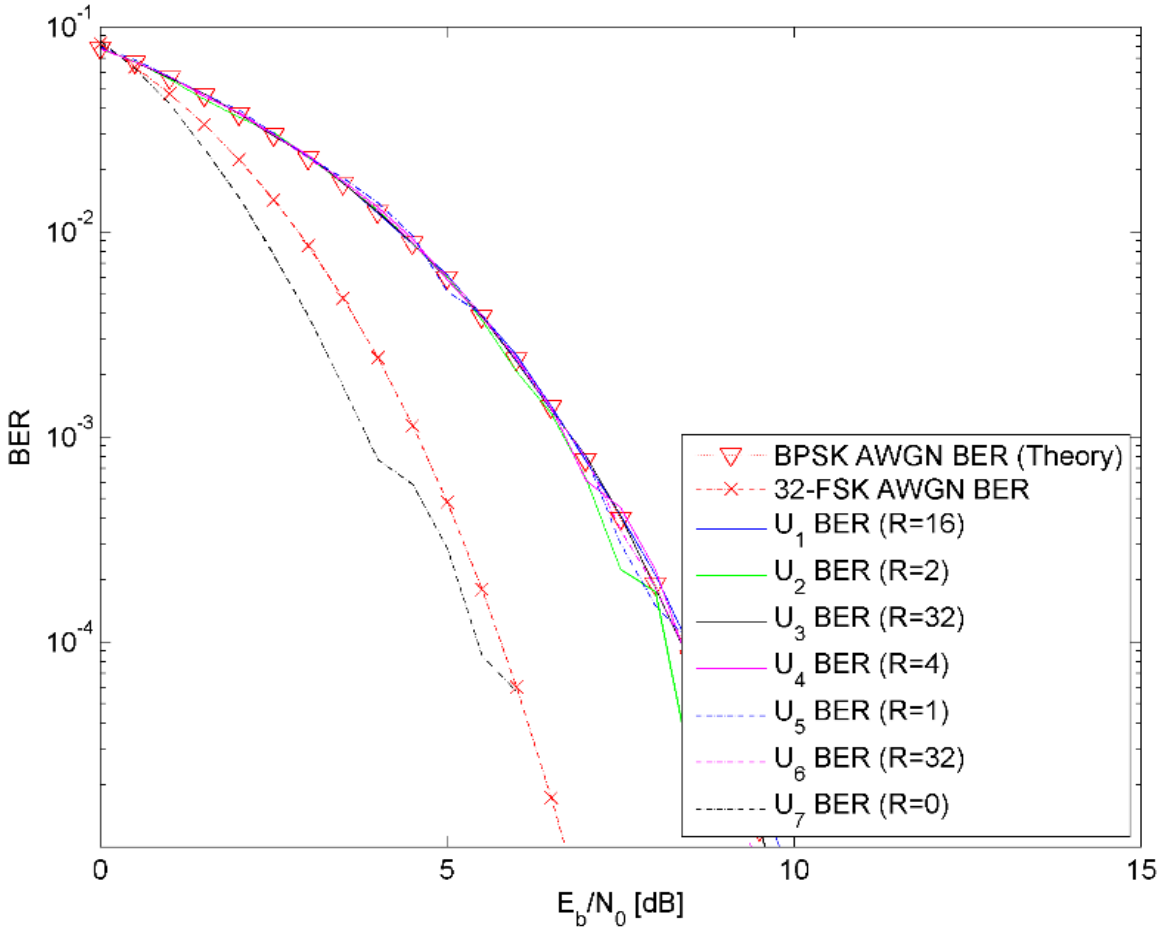

Figure 6.14. Multi-user BER performance of CR-CC-CDMA with randomly selected number of rotations per user (R) and QPSK-CRK (R=0) in a joint system with asynchronous user in AWGN. BER curves for all CR-CC-CDMA users lay on the same line.

For comparison, the multiuser BER performance of a CC-CDMA system using the length 64 low PAPR CCC with one asynchronous user in AWGN is shown in Fig. 6.15. It should be observed that the BER performance of both configurations remain unaffected, in a joint system with an asynchronous user in AWGN, for all users. The BER performance of the users configured for CR-CC-CDMA remains on the theoretical curve for BPSK in AWGN. The BER performance of the user configured for QPSK-CRK is 3.5 dB better than the theoretical curve for BPSK in AWGN and approximately 1 dB better than 32-FSK at 10^{-4} BER probability.

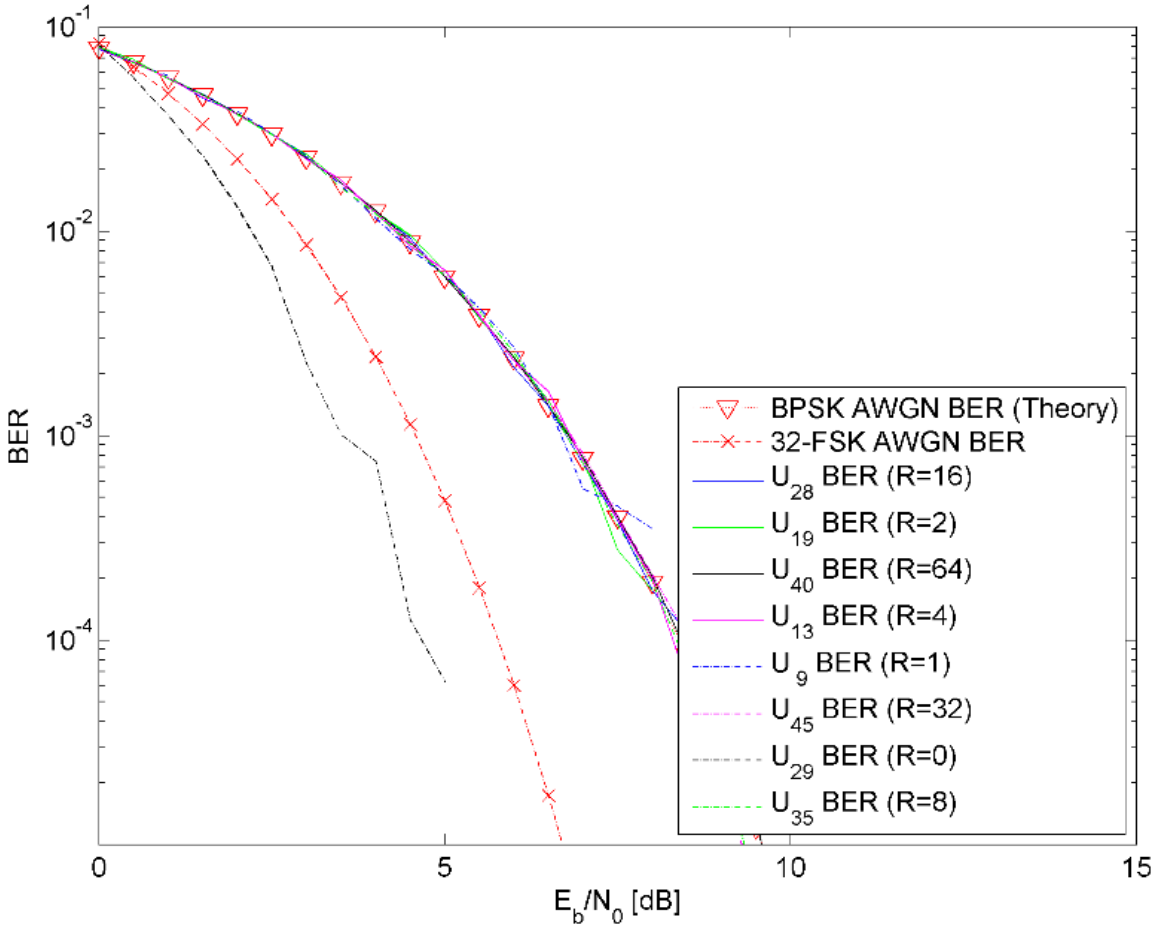

Figure 6.15. Multi-user BER performance of CR-CC-CDMA with randomly selected number of rotations per user (R) and QPSK-CRK (R=0) in a joint system with asynchronous user in AWGN. BER curves for all CR-CC-CDMA users lay on the same line. Note BER reduction for U_{29} when compared to Fig. 6.14.

6.4 CHAPTER SUMMARY

In summary, it was found that the PAPR of the CR-CC-CDMA configuration increased in proportion to the number of rotations used, and thus the SE per user. The PAPR of the QPSK-CRK configuration remained at 3 dB while offering an improvement in SE per user over conventional CC-CDMA. The BER performance of the CR-CC-CDMA configuration remained on the theoretical curve for BPSK in AWGN even in the presence of an asynchronous user. The BER results of the QPSK-CRK configuration offers an

improvement over 32-FSK even in the presence of an asynchronous user. The joint use of both configurations in a CC-CDMA system did not introduce any BER degradation.

CHAPTER 7 DISCUSSION

7.1 CHAPTER OVERVIEW

In Section 7.2 the PAPR results from Section 6.2 are analysed and discussed. In Section 7.3 the BER results from Section 6.3 are analysed and discussed.

7.2 PEAK-TO-AVERAGE POWER RATIO RESULTS

7.2.1 Cyclic rotation complete complementary code division multiple access system

From the PAPR performance results of the CR-CC-CDMA configuration (in Section 6.2.1) it can be concluded that the PAPR of the CR-CC-CDMA configuration is dependent on the number of rotations used per user. This is due to the multiple independent signals that are added together to create the transmitted signal. The PAPR of the CR-CC-CDMA configuration is better than an OFDM system with a comparable IFFT length. This is significant, as many systems employ OFDM modulation with TDMA for multiple access. The inclusion of ACE in a CR-CC-CDMA configuration using a low PAPR CCC shows a minimal increase in PAPR performance. Additionally, the PAPR performance increase is proportional to the number of rotations used per user. This is due to the fact that ACE requires many degrees of freedom to find an optimal solution, which is not possible in a CDMA system, as the resources are distributed between users.

7.2.2 Quadrature phase shift keying complementary rotation keying system

From Fig. 6.4 it was observed that the PAPR of the QPSK-CRK configuration remains at 3 dB for all users. This is due to the intrinsic low PAPR of the CCC used. This is significant as the SE of the QPSK-CRK configuration is significantly higher than a conventional CC-CDMA system.

7.2.3 Joint system performance

From Fig. 6.5 it was observed that the QPSK-CRK configuration offers an improvement in both PAPR and SE over the CR-CC-CDMA configuration using the length 32 CCC using two rotations. The CR-CC-CDMA configuration using more than four rotations offers higher SE than is possible with the QPSK-CRK configuration. The PAPR increases of the

CR-CC-CDMA configuration using two or more rotations is higher than the PAPR of the QPSK-CRK configuration, and increases in proportion to the number of rotations used. The QPSK-CRK configuration using the length 32 low PAPR CCC has a SE of 7/256 bits/s/Hz/user at a PAPR of 3 dB, while the CR-CC-CDMA configuration has a SE of 2/256 bits/s/Hz/user at a PAPR of 3 dB or 8/256 bits/s/Hz/user at a PAPR of 6 dB. This allows a design trade-off to be made between PAPR and SE performance.

7.2.4 Discrete Fourier transform spread orthogonal frequency division multiplexing system

The DFT-s OFDM system offers a significant improvement in PAPR over OFDMA systems. The improvement increases with FFT length. The PAPR of the DFT-s OFDM system for different configurations is nearly constant, thus not allowing the system to adapt to different PAPR requirements. The PAPR of DFT-s OFDM is lower that the PAPR of CR-CC-CDMA with comparable SE, but higher that the PAPR of QPSK-CRK.

7.3 BIT ERROR RATE RESULTS

7.3.1 Cyclic rotation complete complementary code division multiple access system

From Section 6.3, the BER performance of the CR-CC-CDMA configuration in AWGN remains on the theoretical curve for all users and all numbers of rotations used. This shows that the rotations of a flock are all orthogonal to each other, and that the rotations of all the different users are all orthogonal to each other. It has also been shown that all the possible rotations of all the different users remain orthogonal to each other even in the event of an asynchronous user. This is due to the perfect correlation properties of the CCCs used.

7.3.2 Quadrature phase shift keying complementary rotation keying system

It has been shown that the BER performance of the QPSK-CRK configuration in AWGN using the length 32 CCC offers a 1 dB improvement over the upper bound for 32-FSK. The BER of QPSK-CRK decreases as the element sequence length is increased, similarly to M-FSK. The BER results for the different lengths of sequences also correlates with available literature [21].

7.3.3 Joint system performance

It can be seen that the BER performance of all users remain unaffected in a joint system in AWGN. This shows that the rotations of a flock are all orthogonal to each other, and that the rotations of all the different users are all orthogonal to each other. It has also been shown that all the possible rotations of all the different users remain orthogonal to each other even in the event of an asynchronous user. This is due to the perfect correlation properties of the CCCs.

7.4 SPECTRAL EFFICIENCY

Both the CR-CC-CDMA configuration and the QPSK-CRK configuration offer improvements in SE over a conventional CC-CDMA system. The CR-CC-CDMA configuration yielded a scalable SE improvement at the expense of PAPR. The QPSK-CRK configuration yielded a fixed SE improvement, with no increase in PAPR.

A comparison of the SE and PAPR of the CC-CDMA system for the different configurations in Chapter 6 using the length 32 low PAPR CCC is shown in Table 7.1. It should be observed that the SE of the CR-CC-CDMA configuration increases in proportion to the PAPR. The QPSK-CRK configuration provides a SE comparable to the CR-CC-CDMA configuration with 4 rotation at a PAPR of 3 dB, which is a 3 dB PAPR improvement over the CR-CC-CDMA configuration.

7.5 CHAPTER SUMMARY

It has been found that the PAPR of the CR-CC-CDMA configuration is dependent on the number of rotations used per user, and thus on the SE per user. It was found that the CRK configuration provided an improvement in SE over a conventional CC-CDMA system, while maintaining a lowing PAPR than a state of the art MC systems. From the lack of BER degradation, it has been shown that the perfect autocorrelation and cross-correlation properties of the CCCs maintain the BER performance of the CC-CDMA system configured to use both CR-CC-CDMA and CRK, even in the presence of an asynchronous user.

Table 7.1. Spectral efficiency and peak-to-average power ratio comparison. Note the SE and PAPR of QPSK-CRK compared to $\boldsymbol{R = 2}$ and $\boldsymbol{R = 4}$ configurations.

Configuration	SE per User [bits/s/Hz]	SE of system [bits/s/Hz]	PAPR @ $P_{PAPR} = 10^{-2}$ [dB]
QPSK-CRK ($R = 0$)	$\frac{7}{256} \approx 0.027$	$\frac{56}{256} \approx 0.22$	3
CR-CC-CDMA ($R = 1$)	$\frac{2}{256} \approx 0.01$	$\frac{16}{256} \approx 0.06$	3
CR-CC-CDMA ($R = 2$)	$\frac{4}{256} \approx 0.02$	$\frac{32}{256} \approx 0.13$	6
CR-CC-CDMA ($R = 4$)	$\frac{8}{256} \approx 0.03$	0.25	6
CR-CC-CDMA ($R = 8$)	$\frac{16}{256} \approx 0.06$	0.5	8
CR-CC-CDMA ($R = 16$)	$\frac{32}{256} \approx 0.13$	1	9.5
CR-CC-CDMA ($R = 32$)	0.25	2	10.5

CHAPTER 8 CONCLUSION

8.1 CHAPTER OVERVIEW

In Section 8.2 some conclusions are made from the results of the CR-CC-CDMA configuration shown in Section 6.2 and Section 6.3. In Section 8.3 some conclusions are made from the results of the QPSK-CRK configuration shown in Section 6.2 and Section 6.3.

8.2 CYCLIC ROTATION COMPLETE COMPLEMENTARY CODE DIVISION MULTIPLE ACCESS SYSTEM

The PAPR of the CR-CC-CDMA configuration has been shown to be dependent on the number of rotations used per user. This allows dynamic configuration of the system to adjust the number of rotation used per user based on the SE and PAPR requirements for that user. The BER performance of the CR-CC-CDMA configuration has been shown to remain on the theoretical curve for BPSK in AWGN. From this it can be concluded that the CR-CC-CDMA configuration does not cause MUI in AWGN. It has also been shown that the presence of an asynchronous does not degrade the BER performance of the system.

The scalability of SE with PAPR allows this system to be implemented in rural areas, where the low PAPR configurations would allow an increase in the area covered by the system, whilst providing high SE to those users that do not require low PAPR transmission.

8.3 QUADRATURE PHASE SHIFT KEYING COMPLEMENTARY ROTATION KEYING SYSTEM

The PAPR of the QPSK-CRK configuration has been shown to remain at 3 dB, the same as a conventional CC-CDMA system using low PAPR CCCs. The QPSK-CRK configuration has an increased SE compared to a conventional CC-CDMA system without any increase in PAPR, at the cost of minimal complexity. The BER performance of the QPSK-CRK configuration offers a significant improvement over the theoretical curve for BPSK in AWGN, and an improvement on the upper bound for M-FSK when $M = L_E$. This is due to

the increased number of bits per symbol offered by the additional QPSK modulation symbol. The BER curves for different element sequence lengths closely follows the upper bound for M-FSK where $M = L_E * 4$. This can be attributed to these systems having the same number of bits per symbol.

The low PAPR and BER of QPSK-CRK configuration allows CRK systems to be implemented in rural areas, as both factors can be used to increase the area covered by the system. Alternatively, the low PAPR allows transmitters to be implemented using PAs with lower peak power ratings. This can be used to reduce the cost of the transmission equipment required to provide service to an area.

8.4 JOINT SYSTEM

It has been shown that the CR-CC-CDMA and QPSK-CRK configurations can be used as configurations for different users within the same CC-CDMA system. This allows for the greatest level of dynamic configuration based on individual user requirements. The QPSK-CRK configuration offers improved PAPR, BER and SE when compared to low numbers of rotations in CR-CC-CDMA. The assignment to the CR-CC-CDMA configuration is only recommended when a user does not require a low PAPR, in order to provide greater SE.

The flexibility provided by a joint system increases the value of CC-CDMA systems if implemented in a rural area. The QPSK-CRK configuration can be used to provide increased SE over the low PAPR configurations of the CR-CC-CDMA configuration, while the CR-CC-CDMA configuration can provide increased SE to users that do not require low PAPR transmission. As the joint system will be operated in high PAPR configurations at times, the PAs used in the transmission equipment must allow higher PA back-off, thus not allowing any cost saving by using PAs with lower power ratings.

8.5 FUTURE WORK

Recommended future research based on this work are:

- Research into the BER performance of CRK under fading and multipath channel conditions.
- Research into the diversity of CRK under multipath conditions.
- Research into or the development of an optimal receiver structure for CRK for fading and multipath channel conditions.
- Research into the extension of CRK into multiple input multiple output, and the PAPR of such a system.

8.6 CHAPTER SUMMARY

The PAPR of the CR-CC-CDMA configuration has been shown to be dependent on the SE per user. It has been found that the CRK configuration provides an increase in SE over conventional CC-CDMA systems, while maintaining the PAPR of a conventional CC-CDMA system. Both configurations can be used in a joint system without BER degradation. As such, a CC-CDMA system configured to use both CR-CC-CDMA and CRK is recommended for providing more economically feasible data communications in rural areas.

REFERENCES

[1] Constitution of the Republic of South Africa, 1996.

[2] United Nations, "Universal Declaration of Human Rights," 10 Decmber 1948. [Online]. Available: http://www.un.org/en/universal-declaration-human-rights/. [Accessed 27 June 2018].

[3] Vodacom-SA, "Vodacom coverage map," Vodacom, December 2017. [Online]. Available: http://www.vodacom.co.za/vodacom/coverage-map. [Accessed 4 December 2017].

[4] Mobile Telephone Networks, "MTN Coverage map," MTN, 2017. [Online]. Available: https://www.mtn.co.za/Pages/Coverage_Map.aspx. [Accessed 4 December 2017].

[5] 3GPP, "3GPP TS 25.213 v10.0.0 Spreading and modulation (FDD)," 3GPP, Valbonne, 2010.

[6] ANSI/IEEE, *IEEE Standard for Information technology - Telecommunications and information exchange between systems - Local and metropolitan are networks - Specific requirements, IEEE Standard 802.11n-2009*, New York: IEEE, 2009.

[7] 3GPP, "3GPP TS 25.211 v12.2.0 Physical channels and mapping of transport channels," 3GPP, Valbonne, 2016.

[8] H. H. Chen, J. F. Yeh and N. Seuhiro, "A multi-carrier CDMA architecture based on orthogonal complementary codes for new generations of wideband wireless communications," *IEEE Commun. Mag.*, vol. 39, no. 10, pp. 126-135, Oct. 2001.

[9] M. J. Golay, "Complementary series," *IRE Trans. Inf. Theory*, vol. 7, no. 2, pp. 82-87, Apr. 1961.

[10] A. M. Merensky, L. P. Linde and J. H. van Wyk, "A Multi-dimensional code-division-multiplexed OFDMA Modem Using Cyclic Rotated Orthogonal Complete Complementary Codes," *SAIEE Africa Research J.*, vol. 103, no. 2, pp. 94-102, Jun. 2012.

[11] S. Masoud and J. G. Proakis, Digital Communications (International Edition), Singapore: McGraw-Hill, 2008.

[12] H. G. Myung, J. Lim and D. J. Goodman, "Single Carrier FDMA for Uplink wireless Transmission," *IEEE Vehicular Technology Mag,* vol. 1, no. 3, pp. 30-38, Sep 2006.

[13] Z. Liu, Y. L. Guan and U. Parampalli, "New complete complementary codes for peak-to-mean power control in multi-carrier CDMA," *IEEE Trans. Commun.,* vol. 62, no. 3, pp. 1105-1113, Mar. 2014.

[14] S. H. Han and J. H. Lee, "An Overview of Peak-to-Average Power Ratio Reduction Techniques for Multicarrier Transmission," *IEEE Wireless Comm.,* vol. 12, no. 2, pp. 56-65, April 2005.

[15] R. O'Neill and L. B. Lopes, "Envelope variations and spectral splatter in clipped multicarrier signals," in *Proc. IEEE PIMRC '95,* Toronto, Canada, 1995.

[16] B. S. Krongold and D. L. Jones, "PAR Reduction in OFDM via Active Constellation Extension," *IEEE Trans. Broadcasting,* vol. 49, no. 3, pp. 258-268, 2003.

[17] N. van der Neut, B. T. Maharaj, F. H. de Lange, G. Gonzalez, F. Gregorio and J. Cousseau, "PAPR reduction in FBMC systems using a smart gradient-project active constellation extension method," in *Proc. Telecommunications (ICT), 2014 21st International Conference on,* Lisbon, May 2014.

[18] J. Tellado, Peak to Average Power Reduction for Multicarrier Modulation, Ph.D. dissertation, Stanford Univ., 1999.

[19] R. W. Bäuml, R. F. Fisher and J. B. Huber, "Reducing the Peak-to-Average Power Ratio of Multicarrier Modulation by Selected Mapping," *Elect. Lett.,* vol. 32, no. 22, pp. 2056-2057, Oct 1996.

[20] J. A. Davis and J. Jedwab, "Peak-to-mean power control in OFDM, Golay ceomplenetary sequences and Reed-Muller codes," *Ieee Trans. Inf. Theory,* vol. 45, no. 7, pp. 2397-2417, Nov. 1999.

[21] J. K. Hwang, Y. L. Chiu and R. L. Chung, "A new class of MC-CDMA systems using cyclic-shift M-ary biorthogonal keying," in *Proc. International Symposium on Intelligent Signal Processing an Communcation Systems,* Tottori, Japan, Dec. 2006.

[22] L. Yang and L. Hanzo, "Multicarrier DS-CDMA: A multiple access scheme for ubiquitous broadband wireless communications," *IEEE Commun. Mag.*, vol. 41, no. 10, pp. 116-124, Oct. 2003.

[23] Y. Tsai, G. Zhang and Z. Wang, "Polyphase codes for uplink OFDM-CDMA systems," *IEEE Trans. Commun.*, vol. 56, no. 3, pp. 435-444, Mar. 2008.

[24] J.-H. Deng and S.-M. Liao, "A Low-PAPR Multiplexed MC-CDMA System with Enhanced Data Rate over Multipath Channels," in *Proc. 2010 IEEE 71st Vehicular Technology Conference*, Taipei, 2010.

[25] T. Detert, W. Haak and I. Martoyo, "Complete Complementary Codes Applied to UTRA FDD Asynchronous Uplink," in *Proc. IEEE MELCON 2004*, Dubrovnik, Croatia, 2004.

[26] I. Lapin and P. Farkaš, "Peak-to average power ratio of two-dimentional orthogonal complete complementary codes," in *Proc. 58th Int. Symposium ELMAR-2016*, Zadar, Croatia, Sept. 2016.

[27] S.-M. Tseng and M. R. Bell, "Asynchronous Multicarrier DS-CDMA Using," *IEEE Trans. Commun.*, vol. 48, no. 1, pp. 53-59, 2000.

[28] B. M. Popović, "Synthesis of power efficient multitone signals with flat amplitude spectrum," *Ieee Trans. Commun.*, vol. 39, no. 7, pp. 1031-1033, July 1991.

[29] F. G. Paterson, "Generalized Reed-Muller codes and power control in OFDM modulation," *IEEE Trans. Inf. Theory*, vol. 46, no. 1, pp. 104-120, Jan. 2000.

[30] A. Rathinakumar and A. K. Chaturvedi, "Complete mutually orthogonal Golay complementary sets from Reed-Muller codes," *IEEE Trans. Inf. Theory*, vol. 54, no. 3, pp. 1339-1346, Mar. 2008.

[31] B. Horváth, Z. Kollár and P. Horváth, "Bridging the Gap Between Optimal and Suboptimal ACE PAPR Reduction Scheme for OFDM," in *Proc. 24th International Conference Radioelektronika*, Bratislava, 2014.

ADDENDUM A LOW PAPR COMPLETE COMPLEMANTARY CODE SET

The set of low PAPR CCCs used for the simulations in this research are given in modulo 4 notation in Table A.1.

Table A.1. Low peak-to-average power ratio complete complementary codes.

$\boldsymbol{C}_0$	0 1 0 3 0 2 2 2 3 3 2 0 2 3 3 2 2 1 2 3 0 0 2 0 2 0 1 1 3 2 0 1
	2 3 2 1 0 2 2 2 1 1 0 2 2 3 3 2 0 3 0 1 0 0 2 0 0 2 3 3 3 2 0 1
	0 1 0 3 0 2 2 2 1 1 0 2 0 1 1 0 2 1 2 3 0 0 2 0 0 2 3 3 1 0 2 3
	0 1 0 3 2 0 0 0 1 1 0 2 2 3 3 2 2 1 2 3 2 2 0 2 0 2 3 3 3 2 0 1
	0 1 2 1 0 2 0 0 3 3 0 2 2 3 1 0 2 1 0 1 0 0 0 2 2 0 3 3 3 2 2 3
	0 1 2 1 2 0 2 2 3 3 0 2 0 1 3 2 2 1 0 1 2 2 2 0 2 0 3 3 1 0 0 1
	0 1 2 1 0 2 0 0 1 1 2 0 0 1 3 2 2 1 0 1 0 0 0 2 0 2 1 1 1 0 0 1
	2 3 0 3 0 2 0 0 3 3 0 2 0 1 3 2 0 3 2 3 0 0 0 2 2 0 3 3 1 0 0 1
$\boldsymbol{C}_1$	0 1 0 3 2 0 0 0 3 3 2 0 0 1 1 0 2 1 2 3 2 2 0 2 2 0 1 1 1 0 2 3
	2 3 2 1 2 0 0 0 1 1 0 2 0 1 1 0 0 3 0 1 2 2 0 2 0 2 3 3 1 0 2 3
	0 1 0 3 2 0 0 0 1 1 0 2 2 3 3 2 2 1 2 3 2 2 0 2 0 2 3 3 3 2 0 1
	0 1 0 3 0 2 2 2 1 1 0 2 0 1 1 0 2 1 2 3 0 0 2 0 0 2 3 3 1 0 2 3
	0 1 2 1 2 0 2 2 3 3 0 2 0 1 3 2 2 1 0 1 2 2 2 0 2 0 3 3 1 0 0 1
	0 1 2 1 0 2 0 0 3 3 0 2 2 3 1 0 2 1 0 1 0 0 0 2 2 0 3 3 3 2 2 3
	0 1 2 1 2 0 2 2 1 1 2 0 2 3 1 0 2 1 0 1 2 2 2 0 0 2 1 1 3 2 2 3
	2 3 0 3 2 0 2 2 3 3 0 2 2 3 1 0 0 3 2 3 2 2 2 0 2 0 3 3 3 2 2 3

C_2	0 1 0 3 0 2 2 2 1 1 0 2 0 1 1 0 2 1 2 3 0 0 2 0 0 2 3 3 1 0 2 3
	2 3 2 1 0 2 2 2 3 3 2 0 0 1 1 0 0 3 0 1 0 0 2 0 2 0 1 1 1 0 2 3
	0 1 0 3 0 2 2 2 3 3 2 0 2 3 3 2 2 1 2 3 0 0 2 0 2 0 1 1 3 2 0 1
	0 1 0 3 2 0 0 0 3 3 2 0 0 1 1 0 2 1 2 3 2 2 0 2 2 0 1 1 1 0 2 3
	0 1 2 1 0 2 0 0 1 1 2 0 0 1 3 2 2 1 0 1 0 0 0 2 0 2 1 1 1 0 0 1
	0 1 2 1 2 0 2 2 1 1 2 0 2 3 1 0 2 1 0 1 2 2 2 0 0 2 1 1 3 2 2 3
	0 1 2 1 0 2 0 0 3 3 0 2 2 3 1 0 2 1 0 1 0 0 0 2 2 0 3 3 3 2 2 3
	2 3 0 3 0 2 0 0 1 1 2 0 2 3 1 0 0 3 2 3 0 0 0 2 0 2 1 1 3 2 2 3
C_3	0 1 0 3 2 0 0 0 1 1 0 2 2 3 3 2 2 1 2 3 2 2 0 2 0 2 3 3 3 2 0 1
	2 3 2 1 2 0 0 0 3 3 2 0 2 3 3 2 0 3 0 1 2 2 0 2 2 0 1 1 3 2 0 1
	0 1 0 3 2 0 0 0 3 3 2 0 0 1 1 0 2 1 2 3 2 2 0 2 2 0 1 1 1 0 2 3
	0 1 0 3 0 2 2 2 3 3 2 0 2 3 3 2 2 1 2 3 0 0 2 0 2 0 1 1 3 2 0 1
	0 1 2 1 2 0 2 2 1 1 2 0 2 3 1 0 2 1 0 1 2 2 2 0 0 2 1 1 3 2 2 3
	0 1 2 1 0 2 0 0 1 1 2 0 0 1 3 2 2 1 0 1 0 0 0 2 0 2 1 1 1 0 0 1
	0 1 2 1 2 0 2 2 3 3 0 2 0 1 3 2 2 1 0 1 2 2 2 0 2 0 3 3 1 0 0 1
	2 3 0 3 2 0 2 2 1 1 2 0 0 1 3 2 0 3 2 3 2 2 2 0 0 2 1 1 1 0 0 1
C_4	3 0 0 3 3 3 2 0 0 2 2 2 1 2 1 0 2 1 3 0 0 2 3 3 2 2 0 2 1 0 1 2
	3 0 0 3 1 1 0 2 0 2 2 2 3 0 3 2 2 1 3 0 2 0 1 1 2 2 0 2 3 2 3 0
	1 2 2 1 1 1 0 2 0 2 2 2 1 2 1 0 0 3 1 2 2 0 1 1 2 2 0 2 1 0 1 2
	3 0 0 3 1 1 0 2 2 0 0 0 1 2 1 0 2 1 3 0 2 0 1 1 0 0 2 0 1 0 1 2
	3 0 2 1 3 3 0 2 0 2 0 0 1 2 3 2 2 1 1 2 0 2 1 1 2 2 2 0 1 0 3 0
	1 2 0 3 3 3 0 2 2 0 2 2 1 2 3 2 0 3 3 0 0 2 1 1 0 0 0 2 1 0 3 0
	1 2 0 3 1 1 2 0 0 2 0 0 1 2 3 2 0 3 3 0 2 0 3 3 2 2 2 0 1 0 3 0
	1 2 0 3 3 3 0 2 0 2 0 0 3 0 1 0 0 3 3 0 0 2 1 1 2 2 2 0 3 2 1 2

C_5	1 2 2 1 3 3 2 0 2 0 0 0 1 2 1 0 0 3 1 2 0 2 3 3 0 0 2 0 1 0 1 2
	1 2 2 1 1 1 0 2 2 0 0 0 3 0 3 2 0 3 1 2 2 0 1 1 0 0 2 0 3 2 3 0
	3 0 0 3 1 1 0 2 2 0 0 0 1 2 1 0 2 1 3 0 2 0 1 1 0 0 2 0 1 0 1 2
	1 2 2 1 1 1 0 2 0 2 2 2 1 2 1 0 0 3 1 2 2 0 1 1 2 2 0 2 1 0 1 2
	1 2 0 3 3 3 0 2 2 0 2 2 1 2 3 2 0 3 3 0 0 2 1 1 0 0 0 2 1 0 3 0
	3 0 2 1 3 3 0 2 0 2 0 0 1 2 3 2 2 1 1 2 0 2 1 1 2 2 2 0 1 0 3 0
	3 0 2 1 1 1 2 0 2 0 2 2 1 2 3 2 2 1 1 2 2 0 3 3 0 0 0 2 1 0 3 0
	3 0 2 1 3 3 0 2 2 0 2 2 3 0 1 0 2 1 1 2 0 2 1 1 0 0 0 2 3 2 1 2
C_6	1 2 2 1 1 1 0 2 0 2 2 2 1 2 1 0 0 3 1 2 2 0 1 1 2 2 0 2 1 0 1 2
	1 2 2 1 3 3 2 0 0 2 2 2 3 0 3 2 0 3 1 2 0 2 3 3 2 2 0 2 3 2 3 0
	3 0 0 3 3 3 2 0 0 2 2 2 1 2 1 0 2 1 3 0 0 2 3 3 2 2 0 2 1 0 1 2
	1 2 2 1 3 3 2 0 2 0 0 0 1 2 1 0 0 3 1 2 0 2 3 3 0 0 2 0 1 0 1 2
	1 2 0 3 1 1 2 0 0 2 0 0 1 2 3 2 0 3 3 0 2 0 3 3 2 2 2 0 1 0 3 0
	3 0 2 1 1 1 2 0 2 0 2 2 1 2 3 2 2 1 1 2 2 0 3 3 0 0 0 2 1 0 3 0
	3 0 2 1 3 3 0 2 0 2 0 0 1 2 3 2 2 1 1 2 0 2 1 1 2 2 2 0 1 0 3 0
	3 0 2 1 1 1 2 0 0 2 0 0 3 0 1 0 2 1 1 2 2 0 3 3 2 2 2 0 3 2 1 2
C_7	3 0 0 3 1 1 0 2 2 0 0 0 1 2 1 0 2 1 3 0 2 0 1 1 0 0 2 0 1 0 1 2
	3 0 0 3 3 3 2 0 2 0 0 0 3 0 3 2 2 1 3 0 0 2 3 3 0 0 2 0 3 2 3 0
	1 2 2 1 3 3 2 0 2 0 0 0 1 2 1 0 0 3 1 2 0 2 3 3 0 0 2 0 1 0 1 2
	3 0 0 3 3 3 2 0 0 2 2 2 1 2 1 0 2 1 3 0 0 2 3 3 2 2 0 2 1 0 1 2
	3 0 2 1 1 1 2 0 2 0 2 2 1 2 3 2 2 1 1 2 2 0 3 3 0 0 0 2 1 0 3 0
	1 2 0 3 1 1 2 0 0 2 0 0 1 2 3 2 0 3 3 0 2 0 3 3 2 2 2 0 1 0 3 0
	1 2 0 3 3 3 0 2 2 0 2 2 1 2 3 2 0 3 3 0 0 2 1 1 0 0 0 2 1 0 3 0
	1 2 0 3 1 1 2 0 2 0 2 2 3 0 1 0 0 3 3 0 2 0 3 3 0 0 0 2 3 2 1 2